# Aberrant induction of LMO2 by the E2A-HLF chimeric transcription factor and its implication in leukemogenesis of B-precursor ALL with t(17;19)

Kinuko Hirose,[1] Takeshi Inukai,[1] Jiro Kikuchi,[2] Yusuke Furukawa,[2] Tomokatsu Ikawa,[3] Hiroshi Kawamoto,[3] S. Helen Oram,[4] Berthold Göttgens,[4] Nobutaka Kiyokawa,[5] Yoshitaka Miyagawa,[5] Hajime Okita,[5] Koshi Akahane,[1] Xiaochun Zhang,[1] Itaru Kuroda,[1] Hiroko Honna,[1] Keiko Kagami,[1] Kumiko Goi,[1] Hidemitsu Kurosawa,[6] A. Thomas Look,[7] Hirotaka Matsui,[8] Toshiya Inaba,[8] and Kanji Sugita[1]

[1]Pediatrics, School of Medicine, University of Yamanashi, Yamanashi, Japan; [2]Stem Cell Regulation, Center for Molecular Medicine, Jichi Medical School, Tochigi, Japan; [3]Laboratory for Lymphocyte Development, RIKEN Research Center for Allergy and Immunology, Yokohama, Japan; [4]Department of Haematology, Cambridge Institute for Medical Research, Cambridge University, Cambridge, United Kingdom; [5]Developmental Biology, National Research Institute for Child Health and Development, Tokyo, Japan; [6]Department of Pediatrics, Dokkyo Medical School, Tochigi, Japan; [7]Pediatric Oncology, Dana-Farber Cancer Institute, Boston, MA; and [8]Molecular Oncology, Research Institute for Radiation Biology and Medicine, Hiroshima University, Hiroshima, Japan

**LMO2, a critical transcription regulator of hematopoiesis, is involved in human T-cell leukemia. The binding site of proline and acidic amino acid–rich protein (PAR) transcription factors in the promoter of the *LMO2* gene plays a central role in hematopoietic-specific expression. E2A-HLF fusion derived from t(17;19) in B-precursor acute lymphoblastic leukemia (ALL) has the transactivation domain of E2A and the basic region/leucine zipper domain of HLF, which is a PAR transcription factor, raising the possibility that E2A-HLF aberrantly induces LMO2 expression. We here demonstrate that cell lines and a primary sample of t(17;19)-ALL expressed LMO2 at significantly higher levels than other B-precursor ALLs did. Transfection of *E2A-HLF* into a non-t(17;19) B-precursor ALL cell line induced *LMO2* gene expression that was dependent on the DNA-binding and transactivation activities of E2A-HLF. The PAR site in the *LMO2* gene promoter was critical for E2A-HLF-induced LMO2 expression. Gene silencing of *LMO2* in a t(17;19)-ALL cell line by short hairpin RNA induced apoptotic cell death. These observations indicated that E2A-HLF promotes cell survival of t(17;19)-ALL cells by aberrantly up-regulating LMO2 expression. LMO2 could be a target for a new therapeutic modality for extremely chemo-resistant t(17;19)-ALL. (*Blood*. 2010;116(6):962-970)**

## Introduction

Transcription factors that regulate normal hematopoiesis are frequently involved in leukemogenesis[1,2] through 2 types of chromosomal translocation: one causes in-frame fusion of 2 genes and the resultant chimeric transcription factor acquires novel functions and/or functionally disrupts the normal gene products, and the other causes aberrant activation of a transcription factor gene due to juxtaposition to a strong enhancer of the immunoglobulin or T-cell receptor (TCR) loci. The *LMO2* gene, located on the short arm of chromosome 11 at band 13 (11p13), was discovered from a recurrent site of translocations in T-cell acute lymphoblastic leukemia (T-ALL) as a paradigm of the latter type of translocation.[3,4] LMO2 is a member of the LIM-only zinc finger protein family and is present in a transcription factor complex[5] that also includes E2A, TAL1, GATA1, and LDB1 in erythroid cells.[6] Within this complex, LMO2 mediates the protein-protein interactions by recruiting LDB1,[7] whereas TAL1, GATA1, and E2A directly bind to the specific DNA target sites.[6,8] Homozygous null mutation of *Lmo2* showed embryonic lethality due to lack of yolk sac erythropoiesis,[9] and chimeric animals produced from homozygous-deficient embryonic stem cells demonstrated a requirement of *Lmo2* in adult hematopoiesis[10] and angiogenic remodeling of the vasculature.[11] *Lmo2* is expressed in long-term repopulating hematopoietic stem cells[12] and in hematopoietic progenitors,[9] and its expression is maintained in erythroid cells during differentiation. In contrast, *Lmo2* expression is repressed in terminally differentiated granulocytes, macrophages, T cells, and B cells[9] with the exception of germinal center B cells.[13-15] During T-cell development, *Lmo2* is expressed in immature CD4/CD8 double-negative thymocytes and is down-regulated as maturation progresses,[16] and transgenic mice expressing *Lmo2* using a thymocyte-specific promoter developed an accumulation of CD4/CD8 double-negative thymocytes and eventually a T-cell lymphoma.[17-20] Of note, among X-linked severe combined immunodeficiency patients receiving retroviral *IL2Rγc* gene therapy, 2 patients developed T-ALL due to aberrant activation of *LMO2* via integration of the retroviral vector in the *LMO2* gene.[16,21,22] These observations suggested that deregulated *LMO2* increases susceptibility to T-cell malignancies by blocking differentiation. Although similar down-regulation of LMO2 was suggested during B-cell development,[9] the significance of LMO2 expression in B-precursor ALL remains totally unclarified.

The *LMO2* gene has 2 transcriptional promoters and comprises 6 exons, of which exons 4, 5, and 6 encode the protein.[23] The distal and proximal promoters are located upstream of exon 1 or 3 of the larger transcripts, respectively, and the 2 resultant transcripts encode the same open reading frame. The proximal promoter is active in hematopoietic progenitor and endothelial cells, dependent

Submitted September 21, 2009; accepted April 15, 2010. Prepublished online as *Blood* First Edition paper, June 2, 2010; DOI 10.1182/blood-2009-09-244673.

The online version of this article contains a data supplement.

The publication costs of this article were defrayed in part by page charge payment. Therefore, and solely to indicate this fact, this article is hereby marked "advertisement" in accordance with 18 USC section 1734.

on activation of 3 conserved Ets sites,[24] but transgenic analysis demonstrated that the proximal promoter alone is insufficient for full expression of the *Lmo2* gene in hematopoietic cells.[24] The distal promoter is involved in hematopoietic-specific *LMO2* gene expression that is dependent on activation of the proline and acidic amino acid-rich protein (PAR) site in the *LMO2* gene promoter.[25] The PAR transcription factors belong to the basic region/leucine zipper (bZIP) factor family and include hepatic leukemic factor (HLF),[26,27] albumin gene promoter D-site binding protein (DBP),[28] and thyrotroph embryonic factor (TEF).[29] Among the PAR transcription factors, it has been demonstrated that TEF shows the highest potential to activate the *LMO2* promoter in erythroid cells.[25]

t(17;19)(q21-q22;p13) is a relatively rare translocation among childhood ALL cases[2] and is linked with the B-precursor phenotype. E2A-HLF derived from t(17;19) promotes anchorage-independent growth of murine fibroblasts[30,31] and protects cells from apoptosis induced by growth factor deprivation,[32-34] and *E2A-HLF* transgenic mice develop T-cell malignancies.[35,36] In E2A-HLF chimera, the transactivation domain of E2A fuses to the bZIP dimerization and DNA-binding domain of HLF, one of the PAR transcription factors.[26,27] As a result, E2A-HLF recognizes the consensus sequence of PAR transcription factors as a dimer and transactivates downstream target genes.[27,31,37,38] Considering the critical involvement of the PAR site in the distal promoter of the *LMO2* gene in the hematopoietic-specific expression of *LMO2*,[25] E2A-HLF might induce aberrant expression of *LMO2* through the distal promoter. In the present study, we show aberrantly higher expression of LMO2 in t(17;19)-ALL as one of the direct targets of E2A-HLF. The biologic significance of LMO2 in leukemogenesis of t(17;19)-ALL is also investigated and discussed.

## Methods

### Leukemia cell lines and patient sample

Four ALL cell lines with 17;19 translocation (UOC-B1, HALO1, YCUB2, Endo-kun) were used in this study. As B-precursor ALL cell lines, 9 *MLL*-rearranged ALL cell lines (KOPN-1, KOPB-26, KOCL-33, -44, -45, -50, -51, -58, and -69),[39] 6 Philadelphia chromosome (Ph1)–positive ALL cell lines (KOPN-30bi, -57bi, -66bi, -72bi, YAMN-73, and -91),[40] 7 t(1;19)-ALL cell lines (697, KOPN-34, -36, -60, -63, YAMN-90, and -92), and 6 other ALL cell lines including 1 with t(12;21) (Reh) and 5 with others (KOPN-35, -61, -62, -79, and -84) were used. Seven T-ALL cell lines (KOPT-K1, -5, -6, -11, YAMT-12, Jurkat, and MOLT4F), 4 Burkitt B-cell lines (KOBK-130, Daudi, Namalwa, and Raji), and 4 Epstein-Barr virus (EBV)–transformed normal B-cell lines (YAMB-1, -3, -4, and -9) were also used. All cell lines were maintained in RPMI1640 medium supplemented with 10% fetal calf serum (FCS) in a humidified atmosphere of 5% $CO_2$ at 37°C. Analysis of a sample from a patient with t(17;19)-ALL was approved by the Ethical Review Board of the University of Yamanashi. Mononuclear cells (blasts > 95%) that had been isolated from bone marrow aspirates of the patient by Ficoll-Hypaque density centrifugation were stored in liquid nitrogen with 15% dimethyl sulfoxide in fetal calf serum (FCS).

### Isolation of normal B precursors

The $CD34^+$ population was separated from human cord blood mononuclear cells (MNCs) using MACS MicroBeads (Miltenyi Biotec) and, subsequently, $CD34^+/CD19^-$ and $CD34^+/CD19^+$ populations were sorted by flow cytometry (FACS Vantage; Becton Dickinson) using FITC-Lineage marker (CD3, CD4, CD8, CD11b, CD56, CD235a, CD41a) in combination with PE-CD34 and APC-CD19. $CD19^+/IgM^-$ and $CD19^+/IgM^+$ populations were sorted from human cord blood MNCs by flow cytometry using FITC-Lineage marker in combination with PE-IgM and APC-CD19. The $CD19^+$ population was also directly separated from peripheral blood MNCs with MACS MicroBeads. RNA was extracted from each population using RNeasy mini kit (QIAGEN), and cDNA was synthesized using SuperScript VILO cDNA synthesis kit (Invitrogen).

### Western blot analysis

Cells were solubilized in Nonidet P-40 lysis buffer, and total cellular proteins were separated by sodium dodecyl sulfate–polyacrylamide gel electrophoresis (SDS-PAGE) under reducing conditions. After transfer onto nitrocellulose membrane and blocking with 5% nonfat dry milk in 0.05% Tween-20 Tris [tris(hydroxymethyl)aminomethane]–buffered saline (TBS), the membrane was incubated with the primary antibodies in 5% milk in TBS. Goat anti–human LMO2 and mouse anti–human α-Tubulin antibodies were purchased from R&D Systems and Sigma-Aldrich, respectively. Rabbit anti–human antibodies against E2A and HLF(C) were established as previously reported.[37] Membranes were incubated with horseradish peroxidase–conjugated rabbit anti–goat, goat anti–mouse, and goat anti–rabbit IgG (1:1000 dilution; MBL) and were then developed using the enhanced chemiluminescence kit (Amersham Pharmacia Biotech).

### Real-time PCR analysis

Total RNA was extracted using Trizol reagent (Invitrogen). Reverse transcription (RT) was performed using random hexamer (Amersham Bioscience) by Superscript II reverse transcriptase (Invitrogen), and then the cDNA product was incubated with RNase (Invitrogen). For quantitative real-time polymerase chain reaction (PCR) of *LMO2*, triplicated samples containing cDNA with Taqman Universal PCR Master Mix (Applied Biosystems) and Gene Expression Product (exons 1/2, HS00951959_m1; exons 4/5, HS00277106_m1; Applied Biosystems) were amplified according to the manufacturer's protocol using KOPT-6 derived from T-ALL with t(11;14) as a control. As an internal control for relative gene expression, quantitative real-time PCR for *GAPDH* (Hs 99999905_m1, Applied Biosystems) was performed.

### Semiquantitative PCR of transcripts derived from distal and proximal promoters

RNA transcripts originating from the distal *LMO2* promoter were quantified with forward primer 5′-CAAAGCAGGCAATTAGCCC-3′ and reverse primer 5′-CCTCTCCACTAGCTACTGC-3′, which are situated in exons 1 and 2, respectively. Total *LMO2* expression was quantified with forward primer 5′- GAGCTGCGACCTCTGTGG-3′ and reverse primer 5′-CACCCGCATTGTCATCTCAT-3′, which are situated in exons 5 and 6, respectively. Standard curves were created against a single copy of the *LMO2* full-length cDNA subcloned into the pGEMT Easy (Promega) backbone. The assay was performed in triplicate, and the mean quantity of proximal promoter-derived transcripts was directly calculated by subtracting the mean quantity of distal promoter-derived transcripts from the mean quantity of total transcripts. To consider the degree of approximation of the calculated mean, the following equation was considered: $\mathrm{var}(a+b) = \mathrm{var}(a)+\mathrm{var}(b)+2\mathrm{cov}(a,b)$. The standard deviation of the quantity of proximal promoter-derived transcripts is therefore assumed to be represented as follows: SD prox LMO2 = sqrt [(SD total LMO2)$^2$- (SD distal LMO2)$^2$].

### Construction of eukaryotic expression vectors and transfection

Expression plasmids containing wild-type and mutated *E2A-HLF* cDNA were constructed with the pMT-$CB6^+$ eukaryotic expression vector (a gift from F. Rauscher III, Wistar Institute, Philadelphia, PA),[32] which contains the inserted cDNA under control of a sheep metallothionein promoter. ΔAD1/ΔLH mutant and Basic region mutant (BX) were prepared as previously reported.[30,33] Transfectants were generated by electroporation followed by selection using neomycin analog G418 as previously reported.[33]

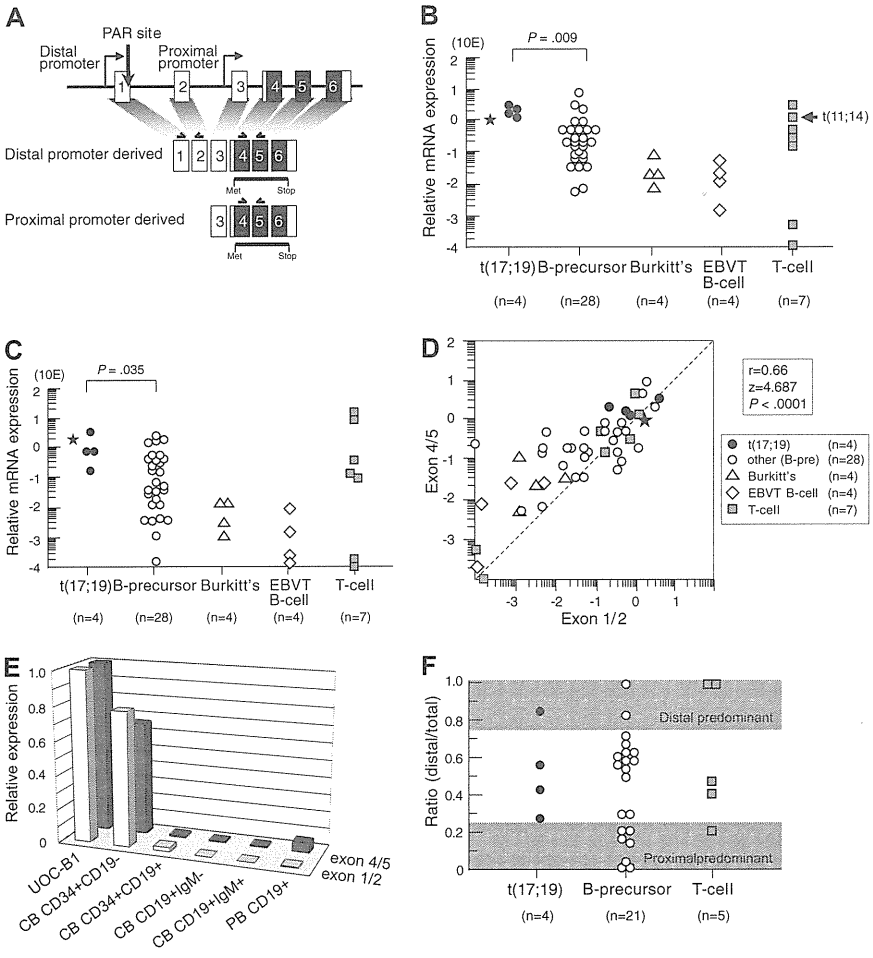


**Figure 1. LMO2 gene expression in t(17;19)-ALL.** (A) Schematic representation of 2 *LMO2* gene promoters and primers for real-time RT-PCR analysis. Primers directed toward exons 1 and 2 specifically detect transcripts derived from the distal promoter, and those directed toward exons 4 and 5 detect transcripts derived from both the distal and proximal promoters. (B) Relative *LMO2* gene expression determined by real-time RT-PCR using the primers for exons 4 and 5. Arrow indicates T-ALL cell line with t(11;14), and asterisk indicates the level of *LMO2* transcripts in a primary leukemia sample from the patient with t(17;19)-ALL. The *P* value determined by Mann-Whitney test is indicated. (C) Relative *LMO2* gene expression determined by real-time RT-PCR using the primers for exons 1 and 2. (D) Correlation between the levels of *LMO2* transcripts quantified by the primers for exons 4 and 5 (vertical axis) and those for exons 1 and 2 (horizontal axis). (E) *LMO2* gene expression in $CD34^+/CD19^-$, $CD34^+/CD19^+$, $CD19^+/IgM^-$, and $CD19^+/IgM^+$ populations of cord blood mononuclear cells (MNCs) and $CD19^+$ population of peripheral blood MNCs. Relative *LMO2* gene expression was determined by real-time RT-PCR using UOC-B1 as a control with the primers for exons 1 and 2 and the primers for exons 4 and 5. The gene expression level of *β-actin* was used as an internal control. SE of triplicated samples was always less than 10%. (F) Ratio of *LMO2* gene expression derived from the distal promoter to total *LMO2* gene expression in ALL cell lines. *LMO2* gene expression in the cell lines that expressed a total *LMO2* gene level of at least 10 times lower than that in UOC-B1 was semiquantifiedby real-time PCR with the specific primers for *LMO2* transcripts sourced at the distal promoter and for total *LMO2* transcripts. The dark areas indicate a proximal promoter-predominant pattern (ratio < 0.25) or a distal promoter-predominant pattern (ratio > 0.75).

### Electrophoretic mobility shift assay

Nuclear extracts of cells were prepared and binding reactions were performed as previously reported.[31,37] Briefly, a $^{32}$P-end-labeled oligonucleotide probe containing wild-type HLF consensus sequence (CS; 5′-GCTACAT*ATTACGTAAT*AAGCGTT-3′) was incubated in 10 μL of binding buffer and 5 μL of nuclear lysates in the presence of 1 μg of shared calf thymus DNA. In the competition inhibition experiments, an approximately 100-fold molar excess of the unlabeled oligonucleotide was added to the reaction mixture. Polyvalent HLF(C) or E2A rabbit antiserum was added to the nuclear lysates before the DNA-binding reaction.

### Reporter assays

−512/+428 *Kpn*I-*Hin*dIII fragment and −512/+249 *Kpn*I/*Bgl*II fragment of the *LMO2* gene generated by PCR were cloned into the pGL3 basic vector (Promega). −512/+428 $PAR^M$ that has the sequence *CATCGAT*-CAT instead of ATTACATCAT in the PAR site was generated by PCR mutagenesis. All constructs were subjected to nucleotide sequence analysis to verify the appropriate insertions. pGL3 control vector and pRL-TK vector were used as the positive control and internal control of transfection efficiency, respectively. For transfection, wild type and E2A-HLF-expressing Nalm6 cells were plated at $5 \times 10^5$ cells/well in a 24-well plate and a total of 5 μg of luciferase reporter plasmid, 1 μg of pRL-TK and 2 μL of lipofectamine (Invitrogen) in 50 μL of serum-free medium (Opti-MEM I; Invirogen) were added. After 24 hours of culture, 100μM $ZnSO_4$ at final concentration was added to induce E2A-HLF expression. Cells were harvested 48 hours after transfection and lysed in 50 μL of lysis buffer (Promega). Activities of firefly and *Renilla* luciferases in each lysate were measured sequentially using the Dual-Luciferase reporter assay system from Promega by a luminometer according to the manufacturer's instructions.

### Lentivirus shRNA/siRNA expression vectors and infection

pLL3.7 lentiviral vector was engineered to produce short hairpin RNAs (shRNAs) under the control of mouse U6 promoter and co-express green fluorescent protein (GFP) as a reporter gene by cytomegalovirus-derived promoter–GFP expression cassette.[41] Short interfering RNA (siRNA) target sequences were designed to be homologous to the wild-type *LMO2* cDNA sequence, and oligonucleotides were subcloned into pLL3.7.[42] The selected sequences were submitted to BLAST search to assure that only *LMO2* was targeted. Among 5 sets of oligonucleotides containing siRNA target sequences, the following set was selected for further analysis due to the specificity and efficiency: 5′-Tgacgcatttcggttgagaa*TTCAAGAGA*Att-ctcaaccgaaatgcgtcTTTTTTC-3′(Blunt-siRNA/sense hairpin-siRNA/anti-sense-polyA-*Xho*I/forward);5′-TCGAGAAAAAAgacgcatttcggttgagaa-TCTCTTGAAttctcaaccgaaatgcgtcA-3′(reverse). The control vector contained the following as ineffective set: 5′-Tgcaatattacatatacgcc*TTCAA-GAGA*ggcgtatatgtaatattgcTTTTTTC-3′ (forward); 5′-TCGAGAAA-AAAgcaatattacatatacgccTCTCTTGAAggcgtatatgtaatattgcA-3′(reverse). pLL3.7 shRNA vector or control vector was cotransfected with packaging vector into 293FT cells and the resulting supernatant was collected after 36 hours.[42] Lentivirus was recovered after ultracentrifugation and infected to UOC-B1 cells.

## Results

### Aberrant expression of LMO2 in t(17;19)-ALL

We first analyzed *LMO2* gene expression in 4 t(17;19)-ALL cell lines, UOC-B1, HALO1, YCUB2, and Endo-kun, by real-time RT-PCR using 2 different sets of primers (Figure 1A): one set

directed toward exons 1 and 2 that is specific for the transcripts derived from the distal promoter, and the other set directed toward exons 4 and 5 that is specific for the transcripts derived from both the distal and proximal promoters. Real-time RT-PCR analysis using the primers specific for exons 4 and 5 demonstrated that all 4 t(17;19)-ALL cell lines expressed *LMO2* transcripts at an equivalent level to that in KOPT6, a T-ALL cell line that aberrantly expresses LMO2 as a result of t(11;14) (Figure 1B). The level of *LMO2* transcripts in t(17;19)-ALL cell lines was significantly higher than that in 28 other B-precursor ALL cell lines ($P = .009$, Mann-Whitney test) including Ph1-ALL, t(1;19)-ALL, and *MLL*+ALL (supplemental Figure 1A, available on the *Blood* Web site; see the Supplemental Materials link at the top of the online article). Real-time RT-PCR analysis using the primers specific for exons 1 and 2 demonstrated that the level of *LMO2* transcripts derived from the distal promoter in t(17;19)-ALL cell lines was also significantly higher than that in the other B-precursor ALL cell lines (Figure 1C and supplemental Figure 1B). A strong correlation was observed between the levels of *LMO2* transcripts quantified by the 2 sets of primers among the 47 cell lines ($r = 0.66$, $P < .0001$; Figure 1D). The primary sample from a t(17;19)-ALL patient also demonstrated high levels of *LMO2* transcripts (Figure 1B-C). Consistent with down-regulation of *LMO2* gene expression during the progression of normal B-cell development,[9] the gene expression level of *LMO2* in Burkitt B-cell lines as well as EBV-transformed normal B-cell lines was unanimously low. Thus, the *LMO2* gene expression level during B-cell development was analyzed using fractions of cord blood and peripheral blood MNCs (Figure 1E). The *LMO2* gene expression level in the $CD34^+/CD19^-$ population of cord blood MNCs was almost equivalent to that in UOC-B1, and it was markedly down-regulated in the $CD34^+/CD19^+$ population. This low expression level was sustained in the $CD19^+/IgM^-$ and the $CD19^+/IgM^+$ populations of cord blood MNCs as well as in the $CD19^+$ population of peripheral blood MNCs.

Next, the contribution of the distal promoter was analyzed in those cell lines that expressed the total *LMO2* gene at a level of at least 10 times lower than that in UOC-B1 by real-time PCR using standard curves, which were created against DNA template of the full-length *LMO2* cDNA that was subcloned into the vector as a single copy. The ratio of the quantity of *LMO2* transcripts sourced at the distal promoter to the quantity of total *LMO2* transcripts in the t(17;19)-ALL cell lines was 0.26 to 0.83 (Figure 1F), indicating that both the distal and the proximal promoters contributed to *LMO2* gene expression. None of the 4 t(17;19)-ALL cell lines showed a proximal promoter-predominant pattern (ratio $< 0.25$), while 7 of 21 other B-precursor ALL cell lines and 1 of 5 T-ALL cell lines showed a proximal promoter-predominant pattern.

We next analyzed LMO2 protein expression by Western blotting using α-tubulin expression as an internal control. Consistent with the gene expression level, LMO2 protein was aberrantly expressed in all 4 t(17;19)-ALL cell lines at a similarly high level to that in the T-ALL cell line with t(11;14) (Figure 2A). compared with other B-precursor ALL cell lines (Figure 2B), the t(17;19)-ALL cell lines expressed significantly higher levels of LMO2 protein ($P = .005$, Mann-Whitney test). Consistent with the low gene expression level, protein expression of LMO2 was undetectable in both Burkitt B-cell lines and EBV-transformed normal B-cell lines. Strong correlations were observed between the levels of LMO2 protein and *LMO2* transcripts analyzed by the primers specific for exons 4 and 5 ($r = 0.72$, $P < .0001$, Figure 2C) and those for exons 1 and 2 ($r = 0.42$, $P = .0089$). These observations indicated that t(17;19)-ALL cells aberrantly express LMO2.

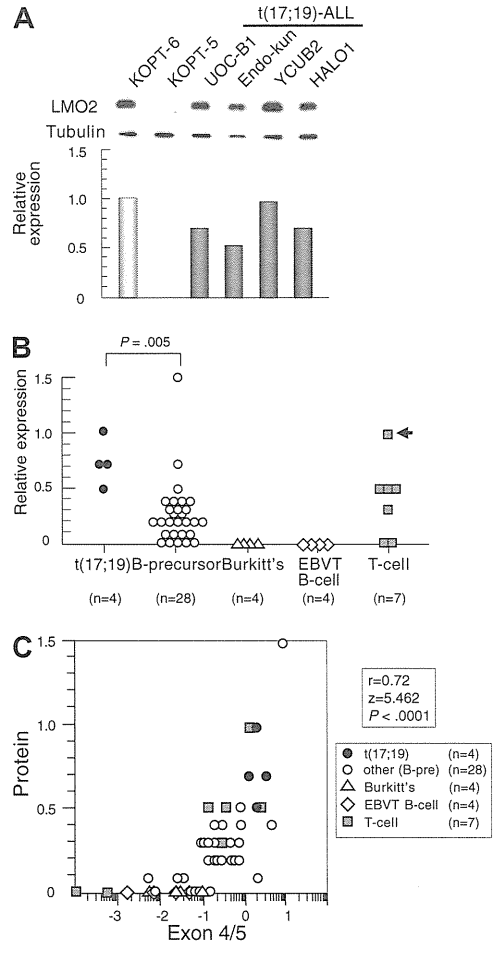


**Figure 2. LMO2 protein expression in t(17;19)-ALL.** (A) Western blot analysis of LMO2. Relative expression of each cell line was determined by quantifying the intensity of each band using KOPT6, a T-ALL cell line with t(11;14), as a positive control and KOPT-5, a T-ALL cell line without LMO2 expression, as a negative control, and normalized by the level of α-tubulin expression as an internal control. (B) Relative level of LMO2 protein expression. The *P* value determined by Mann-Whitney test is indicated. (C) Correlation between levels of relative protein expression of LMO2 (vertical axis) and gene expression of *LMO2* analyzed by real-time RT-PCR using the primers for exons 4 and 5 (horizontal axis).

### Up-regulation of the *LMO2* gene expression by E2A-HLF

To test the possibility that aberrant expression of *LMO2* in t(17;19)-ALL cells is driven by E2A-HLF, we transfected *E2A-HLF* into B-precursor ALL cell line 697, which has t(1;19) and expresses approximately 100-fold lower level of *LMO2* gene than the t(17;19)-ALL cell lines, using a zinc-inducible vector. In E2A-HLF-transfected 697 cells, E2A-HLF was up-regulated to a level equivalent to that in UOC-B1 cells within 4 hours of the addition of zinc to the culture medium (Figure 3A). When analyzed by real-time RT-PCR using primers specific for exons 4 and 5 (Figure 3B), *LMO2* gene expression was up-regulated by the addition of zinc in the E2A-HLF-transfected 697 cells but not in the wild-type 697 cells. When the *LMO2* gene expression derived from the distal and the proximal promoters was differentially semiquantified by real-time PCR (Figure 3C), significant gene expression derived from the distal promoter was immediately induced within 4 hours after the addition of zinc. Subsequently, significant gene expression derived from the proximal promoter was induced within

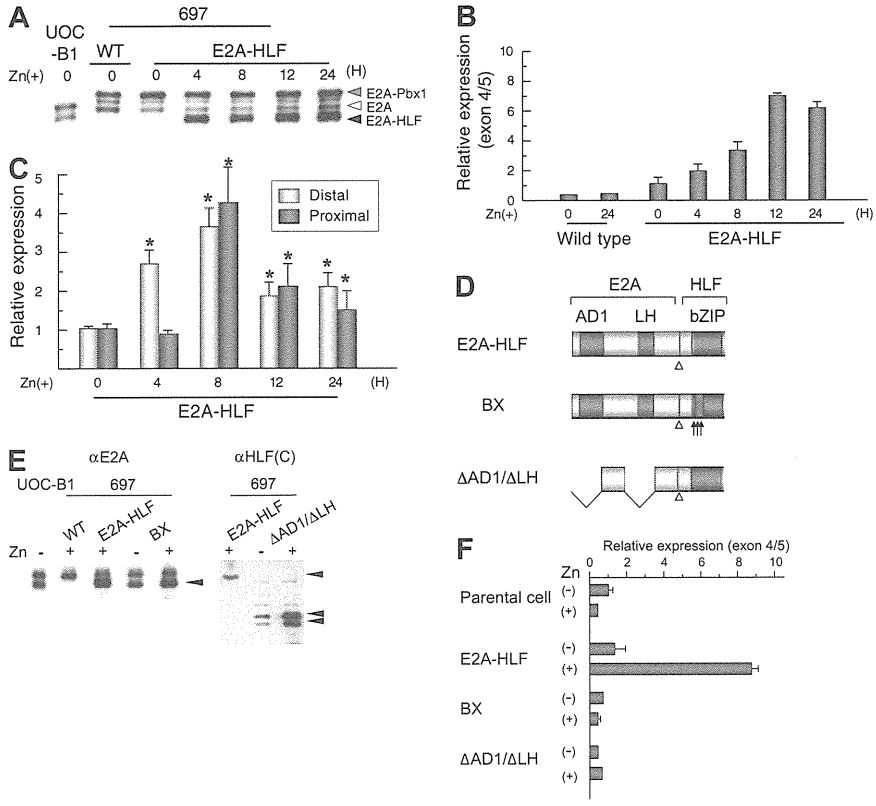


**Figure 3. Induction of *LMO2* gene expression by E2A-HLF.** (A) Induction of E2A-HLF expression. Lysates of wild type (WT) and a clone of *E2A-HLF*–transfected 697 cells as well as UOC-B1 cells harvested at the indicated time after the addition of zinc were blotted with an anti-E2A serum. Gray, white, and black arrowheads indicate E2A-Pbx1, E2A, and E2A-HLF, respectively. (B) Time course analysis of *LOM2* gene expression after induction of E2A-HLF. Levels of *LMO2* transcripts were quantified by real-time RT-PCR using the primers for exons 4 and 5, normalized by *GAPDH* gene expression as an internal control. Changes in fold induction of *LMO2* gene expression level to that in wild type 697 cells cultured in the absence of zinc are shown as the mean ± SE of triplicate samples. (C) Time course analysis of *LOM2* gene expression derived from the distal and proximal promoters after induction of E2A-HLF. Levels of *LMO2* transcripts in E2A-HLF–transfected 697 cells cultured in the presence of zinc were semiquantified by real-time RT-PCR with the specific primers for *LMO2* transcripts sourced at the distal promoter and for total *LMO2* transcripts. Changes in fold induction of *LMO2* gene expression level to that in E2A-HLF–transfected cells cultured in the absence of zinc are shown as the mean ± SE of triplicate samples. Asterisks indicate the significant gene induction determined by t-test. (D) Schematic diagram of mutants of E2A-HLF. (E) Western blot analysis of mutants of E2A-HLF. Lysates of UOC-B1 cells and wild-type (WT) and clones of 697 cells transfected with *E2A-HLF*, *BX*, and *ΔAD1/ΔLH* cultured in the absence or presence of zinc for 24 hours were blotted with E2A (left panel) and HLF(C) (right panel) antisera. (F) *LMO2* gene expression in mutant *E2A-HLF*–transfected 697 cells. Wild-type (WT) and transfectants of 697 cells were cultured in the absence or presence of zinc for 24 hours, and the levels of *LMO2* transcripts were quantified by real-time RT-PCR. Changes in fold induction of *LMO2* gene expression level to that in wild-type 697 cells cultured in the absence of zinc are shown as the mean ± SE of triplicate samples.

8 hours after the addition of zinc. These observations suggest that the distal and the proximal promoters of the *LMO2* gene sequentially contribute to E2A-HLF–induced *LMO2* gene expression. We further tested 2 types of E2A-HLF mutants in 697 cells. BX contains substitutions of 6 critical basic amino acids in the basic region of HLF to abolish DNA-binding ability, while ΔAD1/ΔLH lacks 2 transactivation domains of E2A to abolish transactivation ability but retain DNA-binding ability (Figure 3D).[30,33] Despite almost equivalent levels of expression of each mutant protein to that of E2A-HLF (Figure 3E), the gene expression level of *LMO2* remained unchanged after the addition of zinc (Figure 3F), indicating that both the DNA-binding and transactivation abilities of E2A-HLF are required for induction of *LMO2* gene expression.

### Essential role of the PAR site in the distal promoter of the *LMO2* gene for up-regulation of *LMO2* expression by E2A-HLF

To determine whether E2A-HLF binds to the PAR site in the distal promoter of the *LMO2* gene, we performed electrophoretic mobility shift assay using HLF-CS sequence as a probe in the presence of the double-stranded oligomers listed in Figure 4A as competitors.[25] The DNA-protein complex of E2A-HLF, which was ablated or supershifted in the presence of anti-HLF(C) (Figure 4B lane 1) or anti-E2A (Figure 4B lane 2) antisera, respectively, was competed by the addition of oligomers centered on the PAR site in the distal promoter region (Figure 4B lanes 7-9), although less effectively than unlabeled HLF-CS probe (Figure 4B lanes 3-6). The oligomers containing 2-bp replacement in the 3′ region immediately outside of the PAR site ($PAR^{TG}$) effectively competed the formation of DNA-protein complex (Figure 4B lane 11), while those containing 2-bp ($PAR^{CA}$) or 4-bp ($PAR^{M}$) replacement within the PAR site (Figure 4B lanes 10,12) did not, indicating that the PAR site in the distal promoter of the *LMO2* gene is critical for the binding of E2A-HLF. We also performed electrophoretic mobility shift assay using the sequence of the PAR site in the distal promoter of the *LMO2* gene as a probe, but could not find significant binding (data not shown). High levels of sequence conservation among the mammalian sequences were reported across the entire *LMO2* genomic region.[24] The PAR site sequence in the distal promoter is highly conserved in chimpanzee (*Pan troglodytes*), cow (*Bos Taurus*), and mouse (*Mus musculus*; supplemental Figure 2A), suggesting that the PAR site plays an essential role in the *LMO2* gene expression in these mammalian species. Consistent with conservation of the PAR site in the distal promoter of mouse *lom2* gene, when *E2A-HLF* was transfected into FL5.12 cells, an IL-3–dependent mouse pro-B cell line, using zinc inducible vector as reported before,[33] *lmo2* gene expression derived from the distal

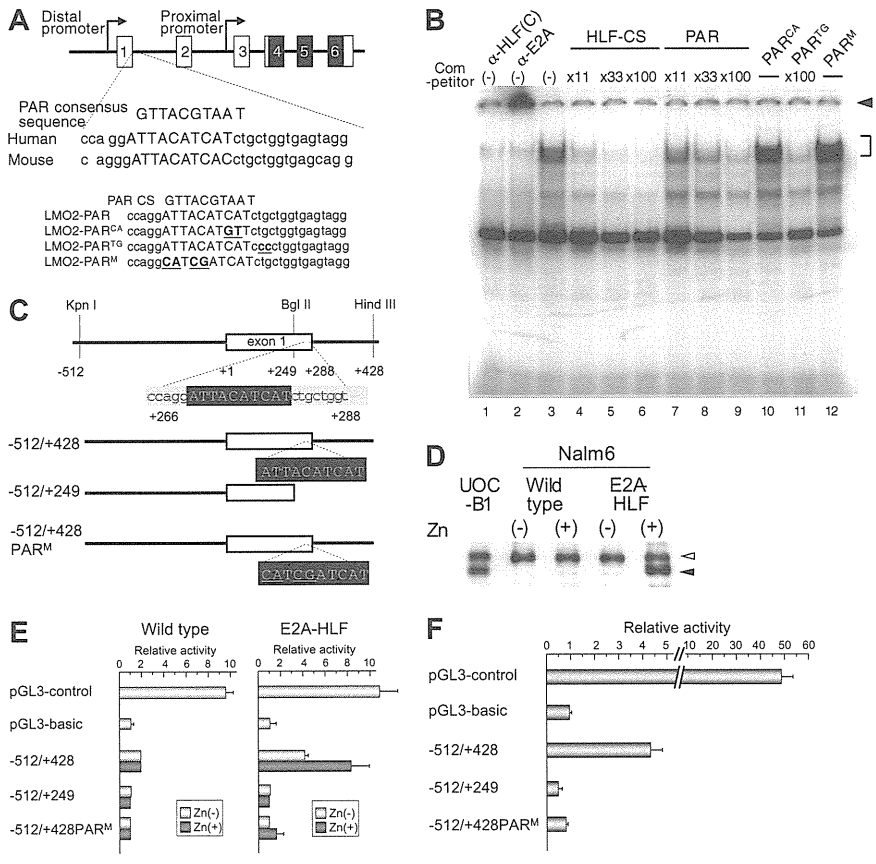


**Figure 4. Involvement of the PAR site in the distal promoter of *LMO2* gene in E2A-HLF–induced LMO2 expression.** (A) Schematic representation of the proline and acidic amino acid–rich protein (PAR) site in the distal promoter of the *LMO2* gene and oligonucleotides used as competitors in electrophoretic mobility shift assay. Mutations in the sequence are underlined. (B) Electrophoretic mobility shift assay performed in nuclear extracts from UOC-B1 cells using an HLF-CS sequence as a probe in the presence of a series of double-stranded oligomers as competitors (lanes 4-12) or anti-HLF(C) (lane 1) and anti-E2A (lane 2) sera. The molar ratio of cold competitor to probe is indicated in each lane. The specific DNA-protein complex is indicated by the bracket and the supershifted complex is indicated by the arrowhead. (C) Schematic representation of 3 reporter constructs for reporter assay. Mutations in the sequence are underlined. (D) Western blot analysis of E2A-HLF–transfected Nalm6 cells. Lysates of UOC-B1 cells and wild type and *E2A-HLF* transfected-Nalm6 cells cultured in the absence or presence of zinc for 24 hours were blotted with E2A antisera. Open and closed arrowheads indicate E2A and E2A-HLF, respectively. (E) Luciferase assay in E2A-HLF–transfected Nalm6 cells. Assays were performed in wild type and E2A-HLF–transfected Nalm6 cells cultured in the absence or presence of zinc for 24 hours after transient transfection of each reporter plasmid. The values were normalized for transfection efficiencies using a cotransfected *Renilla* luciferase construct. (F) Luciferase assay in YCUB2 cells. The values were normalized for transfection efficiencies using a cotransfected *Renilla* luciferase construct.

promoter was up-regulated by the addition of zinc in the *E2A-HLF*-transfected FL5.12 cells but not in the empty vector–transfected FL5.12 cells (supplemental Figure 2B).

We next performed luciferase assay of 3 reporter constructs[25] (Figure 4C) in Nalm6 cells transfected with *E2A-HLF* using a zinc-inducible vector. In E2A-HLF-transfected Nalm6 cells, E2A-HLF was faintly expressed in the absence of zinc, and it was up-regulated in the presence of zinc to a level equivalent to that in UOC-B1 cells (Figure 4D). When the −512/+428 reporter construct was transiently transfected, transcriptional activity was up-regulated in E2A-HLF–transfected Nalm6 cells in the presence of zinc whereas it was virtually silent in the wild-type Nalm6 cells (Figure 4E). Transcriptional activity of the distal promoter was completely abolished by deletion or mutation of the PAR site. Exactly the same pattern of promoter activities was verified in YCUB2, one of the t(17;19)-ALL cell lines (Figure 4F), demonstrating that E2A-HLF up-regulates *LMO2* gene expression by binding to the PAR site in the distal promoter of the *LMO2* gene.

### Induction of apoptosis by shRNA for *LMO2* in a t(17;19)-ALL cell line

To study the significance of aberrant *LMO2* expression in leukemogenesis in t(17;19)-ALL, we introduced shRNA against *LMO2* into the t(17;19)-positive UOC-B1 cell line using a lentivirus vector, which contains *GFP* cDNA for cell sorting (Figure 5A).[41] The expression level of the *LMO2* gene in the GFP-positive (+) population of shRNA virus–infected UOC-B1 (shRNA/UOC-B1) cells was approximately 1000-fold lower than that in the GFP+ control virus–infected UOC-B1 (control/UOC-B1) cells when analyzed by real-time RT-PCR using the primers for exons 4 and 5 (Figure 5B). Despite infection with the same multiplicity of infection, the percentage of the GFP+ population decreased in the shRNA/UOC-B1 cells, in particular the GFP$^{high}$ population that is supposed to express a higher level of shRNA, whereas it was unchanged in the control/UOC-B1 cells (Figure 5C). The percentage of the GFP+ population in shRNA/UOC-B1 cells was significantly lower than that in the control/UOC-B1 cells (Figure 5D, 7.5% vs 30.5% on day 5 after infection; $P = .003$ by $t$ test). By contrast, when infected into 697 cells, a t(1;19)-ALL cell line used as a control, the percentage of the GFP+ population was stable in both the shRNA-virus-infected and the control virus-infected cells (Figure 5C).

To determine whether the reduction in the GFP+ cells in shRNA/UOC-B1 cells was due to cell death or cell-cycle arrest, we performed flow cytometric analysis of BrdU/7-AAD double staining on day 3 after infection (Figure 5E). The percentage of sub-G0/G1 apoptotic cells in the GFP+ shRNA/UOC-B1 cells was significantly higher than that in the control/UOC-B1 cells (12.4% vs 3.6%; $P = .014$ by $t$ test, Figure 5F), while the percentages of cells in the G0/G1, S, and G2/M phases were almost unchanged. Moreover, as shown in Figure 5G, the percentage of caspase-3–activated cells in the GFP+ shRNA/UOC-B1 cells was significantly higher than that in the control/UOC-B1 cells (21.4% vs 0.5%; $P = .00087$ by $t$ test). These observations demonstrate that induction of apoptotic cell death is responsible for the reduction in the GFP+ population among shRNA/UOC-B1 cells.

## Discussion

In T-ALL, 2 mechanisms of aberrant expression of the *LMO2* gene have been well characterized: one is translocation of the *LMO2* gene, leading to its combination with enhancers or other regulatory elements of *TCR* genes,[1,3,4,43] and the other is cryptic deletion at

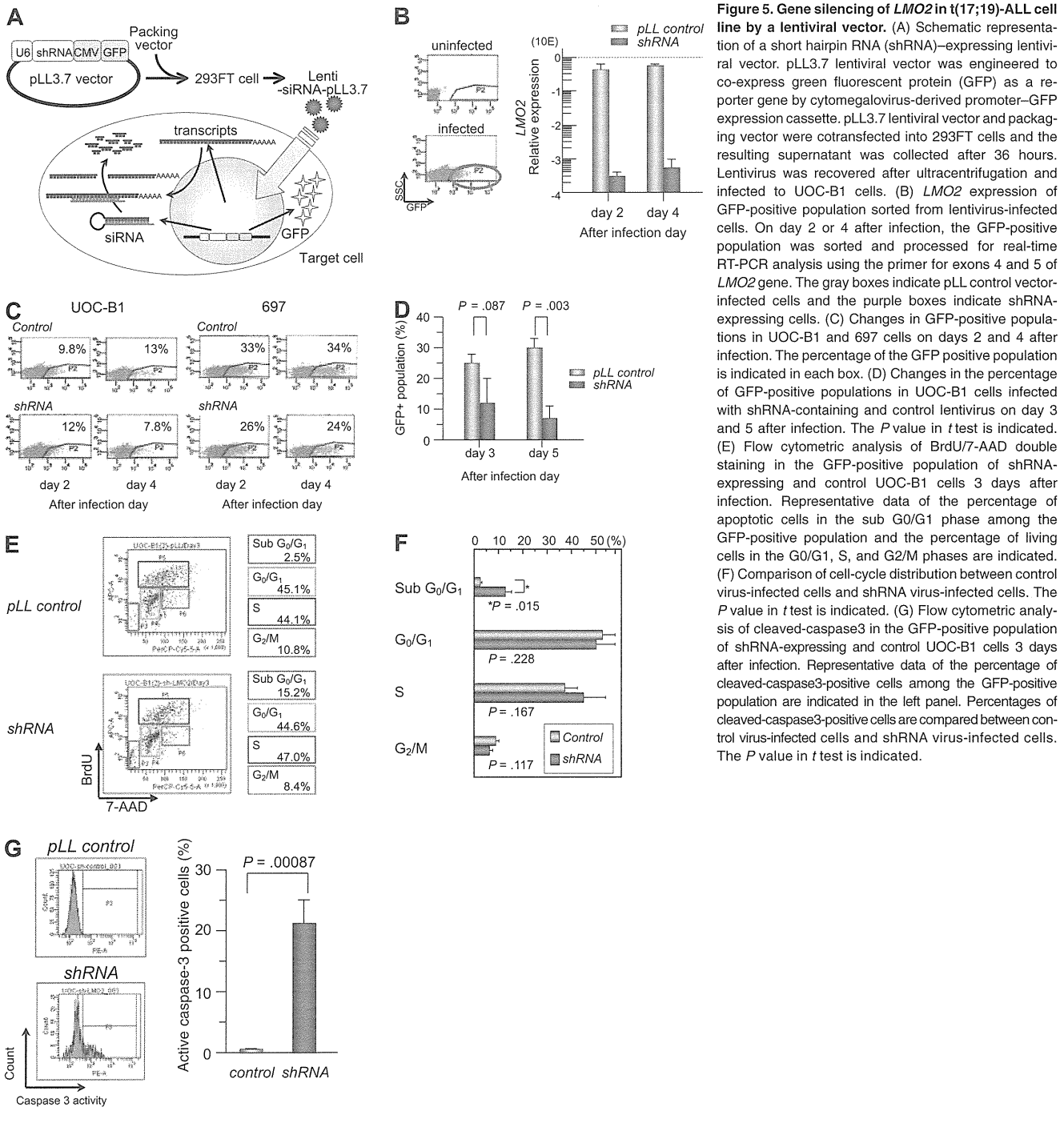


**Figure 5. Gene silencing of *LMO2* in t(17;19)-ALL cell line by a lentiviral vector.** (A) Schematic representation of a short hairpin RNA (shRNA)–expressing lentiviral vector. pLL3.7 lentiviral vector was engineered to co-express green fluorescent protein (GFP) as a reporter gene by cytomegalovirus-derived promoter–GFP expression cassette. pLL3.7 lentiviral vector and packaging vector were cotransfected into 293FT cells and the resulting supernatant was collected after 36 hours. Lentivirus was recovered after ultracentrifugation and infected to UOC-B1 cells. (B) *LMO2* expression of GFP-positive population sorted from lentivirus-infected cells. On day 2 or 4 after infection, the GFP-positive population was sorted and processed for real-time RT-PCR analysis using the primer for exons 4 and 5 of *LMO2* gene. The gray boxes indicate pLL control vector-infected cells and the purple boxes indicate shRNA-expressing cells. (C) Changes in GFP-positive populations in UOC-B1 and 697 cells on days 2 and 4 after infection. The percentage of the GFP positive population is indicated in each box. (D) Changes in the percentage of GFP-positive populations in UOC-B1 cells infected with shRNA-containing and control lentivirus on day 3 and 5 after infection. The *P* value in *t* test is indicated. (E) Flow cytometric analysis of BrdU/7-AAD double staining in the GFP-positive population of shRNA-expressing and control UOC-B1 cells 3 days after infection. Representative data of the percentage of apoptotic cells in the sub G0/G1 phase among the GFP-positive population and the percentage of living cells in the G0/G1, S, and G2/M phases are indicated. (F) Comparison of cell-cycle distribution between control virus-infected cells and shRNA virus-infected cells. The *P* value in *t* test is indicated. (G) Flow cytometric analysis of cleaved-caspase3 in the GFP-positive population of shRNA-expressing and control UOC-B1 cells 3 days after infection. Representative data of the percentage of cleaved-caspase3-positive cells among the GFP-positive population are indicated in the left panel. Percentages of cleaved-caspase3-positive cells are compared between control virus-infected cells and shRNA virus-infected cells. The *P* value in *t* test is indicated.

11p12-13 resulting in loss of negative regulatory sequences of the *LMO2* gene.[44] These 2 chromosomal abnormalities directly induce aberrant expression of the *LMO2* gene. Here we demonstrated a novel mechanism for aberrant expression of the *LMO2* gene as a downstream target of E2A-HLF fusion transcript derived from t(17;19) based on the following observations: all 4 t(17;19)-ALL cell lines studied and a patient's sample expressed a high level of *LMO2* gene transcript, and transfection of *E2A-HLF* into 697 cells induced gene expression of *LMO2* that was dependent on the transactivation and DNA-binding activities of E2A-HLF. E2A-HLF specifically bound to the PAR site in the distal promoter of the *LMO2* gene at least in vitro and enhanced promoter activity. Moreover, *LMO2* transcripts derived from both the proximal and distal promoters were expressed in t(17;19)-ALL cell lines. E2A-HLF rapidly induced *LMO2* gene expression originating from the distal promoter, and then induced *LMO2* gene expression derived from the proximal promoter, suggesting that E2A-HLF induces *LMO2* gene expression not only directly through the PAR site in the distal promoter but also indirectly through the proximal promoter.

It has been reported that LMO2 expression is down-regulated during T-cell development at the transition from immature CD4/CD8 double-negative thymocytes to more mature stages[16] and that enforced expression of *LMO2* in thymocytes blocks differentiation of CD4/CD8 double-negative thymocytes and induces T-cell malignancies.[17-20] In the present study, we confirmed that *LMO2* gene expression in both EBV-transformed normal B-cell lines and Burkitt B-cell lines was significantly lower than that in B-precursor ALL cell lines. In particular, LMO2 protein expression was almost

undetectable in these normal and leukemic B-cell lines. Moreover, the *LMO2* gene expression level was markedly down-regulated during the transition from CD19-negative to CD19-positive population in the cord blood $CD34^+$MNCs. These data are in agreement with the down-regulation of *LMO2* gene expression during the early phase in the normal progression of B-cell development.[19] Of note, gene silencing of *LMO2* by the introduction of shRNA using lentivirus vector induced specific cell death. Interestingly, a recent analysis by Natkunam et al[15] demonstrated that the majority of CD10-positive germinal center B cells coexpressed LMO2 while $CD79a^+$ plasma cells lacked LMO2 expression, suggesting the association of LMO2 down-regulation with normal B-cell development. These observations seem to be in agreement with the assumption that aberrant expression of LMO2 is involved in the maturation arrest of t(17;19)-ALL cells at the immature B-precursor stage. Taken together, LMO2 expression is down-regulated during the normal development of both T cells and B cells, and its aberrant expression promotes cell survival of immature lymphocytes, which subsequently contributes to leukemogenesis of both T-ALL and B-precursor ALL. In this context, it should be noted that approximately one-fourth of non-t(17;19) B-precursor ALL cell lines expressed LMO2 at an equivalent level to that in t(17;19)-ALL cell lines, suggesting that LMO2 might also play a role, at least in part, in the leukemogenesis of other types of B-precursor ALL. Finally, considering the dismal outcome of conventional chemotherapy for t(17;19)-ALL cases,[45] the development of new therapeutic modalities is urgently needed. Here we demonstrated that gene silencing of *LMO2* using shRNA specifically induced cell death of t(17;19)-ALL cells. Thus, there is a possibility that aberrantly expressed LMO2 in t(17;19)-ALL might become a possible target for therapy.

## Authorship

Contribution: K.H. performed most of experiments and analyzed the data; T. Inukai designed the project, analyzed the data, and wrote the manuscript; J.K. and Y.F. performed shRNA analysis; T. Ikawa, H. Kawamoto, H. Kurosawa, A.T.L., and H.M. provided tools for analysis; S.H.O., B.G, N.K., Y.M., and H.O. performed gene expression analysis; K.A., X.Z., I.K., H.H., K.K., and K.G. performed analysis of cell line; T. Inaba wrote the manuscript; and K.S. supervised the project and wrote the manuscript.

Conflict-of-interest disclosure: The authors declare no competing financial interests.

Correspondence: Dr Takeshi Inukai, Department of Pediatrics, School of Medicine, University of Yamanashi, 1110 Shimokato, Chuo, Yamanashi 409-3898, Japan; e-mail: tinukai@yamanashi.ac.jp.

## References


1. Rabbitts TH. Chromosomal translocations in human cancer. *Nature.* 1994;372(6502):143-149.
2. Look AT. Oncogenic transcription factors in the human acute leukemias. *Science.* 1997; 278(5340):1059-1064.
3. Boehm T, Foroni L, Kaneko Y, Perutz MF, Rabbitts TH. The rhombotin family of cysteine-rich LIM-domain oncogenes: distinct members are involved in T-cell translocations to human chromosomes 11p15 and 11p13. *Proc Natl Acad Sci U S A.* 1991;88(10):4367-4371.
4. Royer-Pokora B, Loos U, Ludwig WD. TTG-2, a new gene encoding a cysteine-rich protein with the LIM motif, is overexpressed in acute T-cell leukaemia with the t(11;14)(p13;q11). *Oncogene.* 1991;6(10):1887-1893.
5. Wadman I, Li J, Bash RO, et al. Specific in vivo association between the bHLH and LIM proteins implicated in human T cell leukemia. *EMBO J.* 1994;13(20):4831-4839.
6. Wadman IA, Osada H, Grutz GG, et al. The LIM-only protein Lmo2 is a bridging molecule assembling an erythroid, DNA-binding complex which includes the TAL1, E47, GATA-1 and Ldb1/NLI proteins. *EMBO J.* 1997;16(11):3145-3157.
7. Agulnick AD, Taira M, Breen JJ, Tanaka T, Dawid IB, Westphal H. Interactions of the LIM-domain-binding factor Ldb1 with LIM homeodomain proteins. *Nature.* 1996;384(6606):270-272.
8. Grütz GG, Bucher K, Lavenir I, Larson T, Larson R, Rabbitts TH. The oncogenic T cell LIM-protein Lmo2 forms part of a DNA-binding complex specifically in immature T cells. *EMBO J.* 1998; 17(16):4594-4605.
9. Warren AJ, Colledge WH, Carlton MB, Evans MJ, Smith AJ, Rabbitts TH. The oncogenic cysteine-rich LIM domain protein rbtn2 is essential for erythroid development. *Cell.* 1994;78(1):45-57.
10. Yamada Y, Warren AJ, Dobson C, Forster A, Pannell R, Rabbitts TH. The T cell leukemia LIM protein Lmo2 is necessary for adult mouse hematopoiesis. *Proc Natl Acad Sci U S A.* 1998;95(7): 3890-3895.
11. Yamada Y, Pannell R, Forster A, Rabbitts TH. The oncogenic LIM-only transcription factor Lmo2 regulates angiogenesis but not vasculogenesis in mice. *Proc Natl Acad Sci U S A.* 2000;97(1):320-324.
12. Akashi K, He X, Chen J, Iwasaki H, Niu C, Steenhard B, Zhang J, Haug J, Li L. Transcriptional accessibility for genes of multiple tissues and hematopoietic lineages is hierarchically controlled during early hematopoiesis. *Blood.* 2003; 101(2):383-389.
13. Alizadeh AA, Eisen MB, Davis RE, et al. Distinct types of diffuse large B-cell lymphoma identified by gene expression profiling. *Nature.* 2000; 403(6769):503-511.
14. Lossos IS, Czerwinski DK, Alizadeh AA, et al. Prediction of survival in diffuse large-B-cell lymphoma based on the expression of six genes. *N Engl J Med.* 2004;350(18):1828-1837.
15. Natkunam Y, Zhao S, Mason DY, et al. The oncoprotein LMO2 is expressed in normal germinal-center B cells and in human B-cell lymphomas. *Blood.* 2007;109(4):1636-1642.
16. McCormack MP, Forster A, Drynan L, Pannell R, Rabbitts TH. The LMO2 T-cell oncogene is activated via chromosomal translocations or retroviral insertion during gene therapy but has no mandatory role in normal T-cell development. *Mol Cell Biol.* 2003;23(24):9003-9013.
17. Fisch P, Boehm T, Lavenir I, et al. T-cell acute lymphoblastic lymphoma induced in transgenic mice by the RBTN1 and RBTN2 LIM-domain genes. *Oncogene.* 1992;7(12):2389-2397.
18. Larson RC, Fisch P, Larson TA, et al. T cell tumours of disparate phenotype in mice transgenic for Rbtn-2. *Oncogene.* 1994;9(12):3675-3681.
19. Larson RC, Osada H, Larson TA, Lavenir I, Rabbitts TH. The oncogenic LIM protein Rbtn2 causes thymic developmental aberrations that precede malignancy in transgenic mice. *Oncogene.* 1995;11(5):853-862.
20. Neale GA, Rehg JE, Goorha RM. Ectopic expression of rhombotin-2 causes selective expansion of CD4-CD8- lymphocytes in the thymus and T-cell tumors in transgenic mice. *Blood.* 1995;86(8): 3060-3071.
21. Hacein-Bey-Abina S, Von Kalle C, Schmidt M, et al. LMO2-associated clonal T cell proliferation in two patients after gene therapy for SCID-X1. *Science.* 2003;302(5644):415-419.
22. McCormack MP, Rabbitts TH. Activation of the T-cell oncogene LMO2 after gene therapy for X-linked severe combined immunodeficiency. *N Engl J Med.* 2004;350(9):913-922.
23. Royer-Pokora B, Rogers M, Zhu TH, Schneider S, Loos U, Bolitz U. The TTG-2/RBTN2 T cell oncogene encodes two alternative transcripts from two promoters: the distal promoter is removed by most 11p13 translocations in acute T cell leukaemia's (T-ALL). *Oncogene.* 1995;10(7):1353-1360.
24. Landry JR, Kinston S, Knezevic K, Donaldson IJ, Green AR, Gottgens B. Fli1, Elf1, and Ets1 regulate the proximal promoter of the LMO2 gene in endothelial cells. *Blood.* 2005;106(8):2680-2687.
25. Crable SC, Anderson KP. A PAR domain transcription factor is involved in the expression from a hematopoietic-specific promoter for the human LMO2 gene. *Blood.* 2003;101(12):4757-4764.
26. Inaba T, Roberts WM, Shapiro LH, et al. Fusion of the leucine zipper gene HLF to the E2A gene in human acute B-lineage leukemia. *Science.* 1992; 257(5069):531-534.
27. Hunger SP, Ohyashiki K, Toyama K, Cleary ML. Hlf, a novel hepatic bZIP protein, shows altered DNA-binding properties following fusion to E2A in t(17;19) acute lymphoblastic leukemia. *Genes Dev.* 1992;6(9):1608-1620.
28. Mueller CR, Maire P, Schibler U. DBP, a liver-enriched transcriptional activator, is expressed late in ontogeny and its tissue specificity is determined posttranscriptionally. *Cell.* 1990;61(2):279-291.
29. Drolet D, Scully K, Simmons D, et al. TEF, a transcription factor expressed specifically in the anterior pituitary during embryogenesis, defines a new class of leucine zipper proteins. *Genes Dev.* 1991;5(10):1739-1753.
30. Yoshihara T, Inaba T, Shapiro LH, Kato JY, Look AT. E2A-HLF-mediated cell transformation requires both the trans-activation domains of E2A and the leucine zipper dimerization domain of HLF. *Mol Cell Biol.* 1995;15(6):3247-3255.

31. Inukai T, Inaba T, Yoshihara T, Look AT. Cell transformation mediated by homodimeric E2A-HLF transcription factors. *Mol Cell Biol.* 1997;17(3):1417-1424.
32. Inaba T, Inukai T, Yoshihara T, et al. Reversal of apoptosis by the leukaemia-associated E2A-HLF chimaeric transcription factor. *Nature.* 1996;382(6591):541-544.
33. Inukai T, Inaba T, Ikushima S, Look AT. The AD1 and AD2 transactivation domains of E2A are essential for the antiapoptotic activity of the chimeric oncoprotein E2A-HLF. *Mol Cell Biol.* 1998;18(10):6035-6043.
34. Inukai T, Inaba T, Dang J, et al. TEF, an antiapoptotic bZIP transcription factor related to the oncogenic E2A-HLF chimera, inhibits cell growth by down-regulating expression of the common beta chain of cytokine receptors. *Blood.* 2005;105(11):4437-4444.
35. Smith KS, Rhee JW, Naumovski L, Cleary ML. Disrupted differentiation and oncogenic transformation of lymphoid progenitors in E2A-HLF transgenic mice. *Mol Cell Biol.* 1999;19(6):4443-4451.
36. Honda H, Inaba T, Suzuki T, et al. Expression of E2A-HLF chimeric protein induced T-cell apoptosis, B-cell maturation arrest, and development of acute lymphoblastic leukemia. *Blood.* 1999;93(9):2780-2790.
37. Inaba T, Shapiro LH, Funabiki T, et al. DNA-binding specificity and trans-activating potential of the leukemia-associated E2A-hepatic leukemia factor fusion protein. *Mol Cell Biol.* 1994;14(5):3403-3413.
38. Hunger SP, Brown R, Cleary ML. DNA-binding and transcriptional regulatory properties of hepatic leukemia factor (HLF) and the t(17;19) acute lymphoblastic leukemia chimera E2A-HLF. *Mol Cell Biol.* 1994;14(9):5986-5996.
39. Inukai T, Zhang X, Goto M, et al. Resistance of infant leukemia with MLL rearrangement to tumor necrosis factor-related apoptosis-inducing ligand: a possible mechanism for poor sensitivity to antitumor immunity. *Leukemia.* 2006;20(12):2119-2129.
40. Uno K, Inukai T, Kayagaki N, et al. TNF-related apoptosis-inducing ligand (TRAIL) frequently induces apoptosis in Philadelphia chromosome-positive leukemia cells. *Blood.* 2003;101(9):3658-3667.
41. Rubinson DA, Dillon CP, Kwiatkowski AV, et al. A lentivirus-based system to functionally silence genes in primary mammalian cells, stem cells and transgenic mice by RNA interference. *Nat Genet.* 2003;33(3):401-406.
42. Kikuchi J, Shimizu R, Wada T, et al. E2F-6 suppresses growth-associated apoptosis of human hematopoietic progenitor cells by counteracting proapoptotic activity of E2F-1. *Stem Cells.* 2007;25(10):2439-2447.
43. Garcia IS, Kaneko Y, Gonzalez-Sarmiento R, et al. A study of chromosome 11p13 translocations involving TCR beta and TCR delta in human T cell leukaemia. *Oncogene.* 1991;6(4):577-582.
44. Van Vlierberghe P, van Grotel M, Beverloo HB, et al. The cryptic chromosomal deletion del(11)(p12p13) as a new activation mechanism of LMO2 in pediatric T-cell acute lymphoblastic leukemia. *Blood.* 2006;108(10):3520-3529.
45. Inukai T, Hirose K, Inaba T, Kurosawa H, et al. Hypercalcemia in childhood acute lymphoblastic leukemia: frequent implication of parathyroid hormone-related peptide and E2A-HLF from translocation 17;19. *Leukemia.* 2007;21(2):288-296.

# Extensive gene deletions in Japanese patients with Diamond-Blackfan anemia

Madoka Kuramitsu,[1] Aiko Sato-Otsubo,[2] Tomohiro Morio,[3] Masatoshi Takagi,[3] Tsutomu Toki,[4] Kiminori Terui,[4] RuNan Wang,[4] Hitoshi Kanno,[5] Shouichi Ohga,[6] Akira Ohara,[7] Seiji Kojima,[8] Toshiyuki Kitoh,[9] Kumiko Goi,[10] Kazuko Kudo,[11] Tadashi Matsubayashi,[12] Nobuo Mizue,[13] Michio Ozeki,[14] Atsuko Masumi,[1] Haruka Momose,[1] Kazuya Takizawa,[1] Takuo Mizukami,[1] Kazunari Yamaguchi,[1] Seishi Ogawa,[2] Etsuro Ito,[4] and Isao Hamaguchi[1]

[1]Department of Safety Research on Blood and Biological Products, National Institute of Infectious Diseases, Tokyo, Japan; [2]Cancer Genomics Project, Graduate School of Medicine, The University of Tokyo, Tokyo, Japan; [3]Department of Pediatrics and Developmental Biology, Graduate School of Medicine, Tokyo Medical and Dental University, Bunkyo-ku, Tokyo, Japan; [4]Department of Pediatrics, Hirosaki University Graduate School of Medicine, Hirosaki, Japan; [5]Department of Transfusion Medicine and Cell Processing, Tokyo Women's Medical University, Tokyo, Japan; [6]Department of Pediatrics, Graduate School of Medical Sciences, Kyushu University, Fukuoka, Japan; [7]First Department of Pediatrics, Toho University School of Medicine, Tokyo, Japan; [8]Department of Pediatrics, Nagoya University Graduate School of Medicine, Nagoya, Japan; [9]Department of Hematology/Oncology, Shiga Medical Center for Children, Shiga, Japan; [10]Department of Pediatrics, School of Medicine, University of Yamanashi, Yamanashi, Japan; [11]Division of Hematology and Oncology, Shizuoka Children's Hospital, Shizuoka, Japan; [12]Department of Pediatrics, Seirei Hamamatsu General Hospital, Shizuoka, Japan; [13]Department of Pediatrics, Kushiro City General Hospital, Hokkaido, Japan; and [14]Department of Pediatrics, Graduate School of Medicine, Gifu University, Gifu, Japan

**Fifty percent of Diamond-Blackfan anemia (DBA) patients possess mutations in genes coding for ribosomal proteins (RPs). To identify new mutations, we investigated large deletions in the RP genes *RPL5*, *RPL11*, *RPL35A*, *RPS7*, *RPS10*, *RPS17*, *RPS19*, *RPS24*, and *RPS26*. We developed an easy method based on quantitative-PCR in which the threshold cycle correlates to gene copy number. Using this approach, we were able to diagnose 7 of 27 Japanese patients (25.9%) possessing mutations that were not detected by sequencing. Among these large deletions, similar results were obtained with 6 of 7 patients screened with a single nucleotide polymorphism array. We found an extensive intragenic deletion in *RPS19*, including exons 1-3. We also found 1 proband with an *RPL5* deletion, 1 patient with an *RPL35A* deletion, 3 with *RPS17* deletions, and 1 with an *RPS19* deletion. In particular, the large deletions in the *RPL5* and *RPS17* alleles are novel. All patients with a large deletion had a growth retardation phenotype. Our data suggest that large deletions in RP genes comprise a sizable fraction of DBA patients in Japan. In addition, our novel approach may become a useful tool for screening gene copy numbers of known DBA genes. (*Blood*. 2012;119(10): 2376-2384)**

## Introduction

Diamond-Blackfan anemia (DBA; MIN# 105650) is a rare congenital anemia that belongs to the inherited BM failure syndromes, generally presenting in the first year of life. Patients typically present with a decreased number of erythroid progenitors in their BM.[1] A main feature of the disease is red cell aplasia, but approximately half of patients show growth retardation and congenital malformations in the craniofacial, upper limb, cardiac, and urinary systems. Predisposition to cancer, in particular acute myeloid leukemia and osteogenic sarcoma, is also characteristic of the disease.[2]

Mutations in the *RPS19* gene were first reported in 25% of DBA patients by Draptchinskaia et al in 1999.[3] Since that initial finding, many genes that encode large (RPL) or small (RPS) ribosomal subunit proteins were found to be mutated in DBA patients, including *RPL5* (approximately 21%), *RPL11* (approximately 9.3%), *RPL35A* (3.5%), *RPS7* (1%), *RPS10* (6.4%), *RPS17* (1%), *RPS24* (2%), and *RPS26* (2.6%).[4-7] To date, approximately half of the DBA patients analyzed have had a mutation in one of these genes. Konno et al screened 49 Japanese patients and found that 30% (12 of 49) carried mutations.[8] In addition, our data showed that 22 of 68 DBA patients (32.4%) harbored a mutation in ribosomal protein (RP) genes (T.T., K.T., R.W., and E.I., unpublished observation, April 16, 2011). These abnormalities of RP genes cause defects in ribosomal RNA processing, formation of either the large or small ribosome subunit, and decreased levels of polysome formation,[4-6,9-12] which is thought to be one of the mechanisms for impairment of erythroid lineage differentiation.

Although sequence analyses of genes responsible for DBA are well established and have been used to identify new mutations, it is estimated that approximately half of the mutations remain to be determined. Because of the difficulty of investigating whole allele deletions, there have been few reports regarding allelic loss in DBA, and they have only been reported for *RPS19* and *RPL35A*.[3,6,13] However, a certain percentage of DBA patients are thought to have a large deletion in RP genes. Therefore, a detailed analysis of allelic loss mutations should be conducted to determine other RP genes that might be responsible for DBA.

In the present study, we investigated large deletions using our novel approach for gene copy number variation analysis based on quantitative-PCR and a single nucleotide polymorphism (SNP) array. We screened Japanese DBA patients and found 7 patients with a large deletion in an allele in *RPL5*, *RPL35A*, *RPS17*, or *RPS19*. Interestingly, all of these patients with a large deletion had a phenotype of growth retardation, including short stature and

Submitted July 24, 2011; accepted November 15, 2011. Prepublished online as *Blood* First Edition paper, January 18, 2012; DOI 10.1182/blood-2011-07-368662.

The online version of this article contains a data supplement.

The publication costs of this article were defrayed in part by page charge payment. Therefore, and solely to indicate this fact, this article is hereby marked "advertisement" in accordance with 18 USC section 1734.

**Table 1. Primers used for synchronized quantitative-PCR (s-q-PCR) of RPL proteins**

| Gene | Primer name | Sequence | Primer name | Sequence | Size, bp |
|---|---|---|---|---|---|
| RPL5 | L5-02F | CTCCCAAAGTGCTTGAGATTACAG | L5-02R | CACCTTTTCCTAACAAATTCCCAAT | 132 |
| | L5-05F | AGCCCTCCAACCTAGGTGACA | L5-05R | GAATTGGGATGGGCAAGAACT | 102 |
| | L5-17F | TGAACCCTTGCCCTAAAACATG | L5-17R | TCTTGGTCAGGCCCTGCTTA | 105 |
| | L5-19F | ATTGTGCAAACTCGATCACTAGCT | L5-19R | GTGTCTGAGGCTAACACATTTCCAT | 103 |
| | L5-21F | GTGCCACTCTCTTGGACAAACTG | L5-21R | CATAGGGCCAAAAGTCAAATAGAAG | 102 |
| | L5-28F | TCCACTTTAGGTAGGCGAAACC | L5-28R | TCAGATTTGGCATGTACCTTTCA | 102 |
| RPL11 | L11-06F | GCACCCACATGGCTTAAAGG | L11-6R | CAACCAACCCATAGGCCAAA | 102 |
| | L11-20F | GAGCCCCCTTTCTCAGATGATA | L11-20R | CATGAACTTGGGCTCTGAATCC | 109 |
| | L11-22F | TATGTGCAGATAAGAGGGCAGTCT | L11-22R | ATACAGATAAGGAAACTGAGGCAGATT | 98 |
| RPL19 | L19-02F | TGGCCTCTCATAAAGGAAATCTCT | L19-02R | GGAATGCAGGCAAGTTACTCTGTT | 103 |
| | L19-08F | TTTGAAGGCAAGAAATAAGTTCCA | L19-08R | AGCACATCACAGAGTCCAAATAGG | 107 |
| | L19-16F | GGTTAGTTGAAGCAGGAGCCTTT | L19-16R | TGCTAGGGAGACAGAAGCACATC | 102 |
| | L19-19F | GGACCAGTAGTTGTGACATCAGTTAAG | L19-19R | CCCATTTGTAACCCCCACTTG | 106 |
| RPL26 | L26-03F | TCCAAAGAGCTGAGACAGAAGTACA | L26-03R | TCCATCAAGACAACGAGAACAAGT | 102 |
| | L26-16F | TTTGAGAATGCTTGAGAGAAGGAA | L26-16R | TTCCAGCACATGTAAAATCAAGGA | 102 |
| | L26-18F | ATGTTTTAATAAGCCCTCCAGTTGA | L26-18R | GAGAACAGCAAGTTGAAAGGTTCA | 102 |
| | L26-20F | GGGCTTTGCTTGATCACTCTAGA | L26-20R | AGGGAGCCCGAAAACATTTAC | 104 |
| RPL35A | L35A-01F | TGTGGCTTCTATTTTGCGTCAT | L35A-01R | GGAATTACCTCCTTTATTGCTTACAAG | 121 |
| | L35A-07F | TTTCCGTTCTGTCTATTGCTGTGT | L35A-07R | GAACCCTGAGTGGAGGATGTTC | 113 |
| | L35A-17F | GCCCACAACCTCCAGAGAATC | L35A-17R | GGATCACTTGAGGCCAGGAAT | 104 |
| | L35A-18F | TTAGGTGGGCTTTTCAGTCTCAA | L35A-18R | ATCTCCTGATTCCCCAACTTTGT | 102 |
| RPL36 | L36-02F | CCGCTCTACAAGTGAAGAAATTCTG | L36-02R | CTCCCTCTGCCTGTGAAATGA | 102 |
| | L36-04F | TGCGTCCTGCCAGTGTTG | L36-04R | GGGTAGCTGTGAGAACCAAGGT | 105 |
| | L36-17F | CCCCTTGAAAGGACAGCAGTT | L36-17R | TTGGACACCAGGCACAGACTT | 114 |

**Table 2. Primers used for s-q-PCR of RPS proteins**

| Gene | Primer name | Sequence | Primer name | Sequence | Size, bps |
|---|---|---|---|---|---|
| RPS7 | S7-11F | GCGCTGCCAGATAGGAAATC | S7-11R | TTAGGGAGCTGCCTTACATATGG | 102 |
| | S7-12F | ACTGGCAGTTCTGTGATGCTAAGT | S7-12R | ACTCTTGCTCATCTCCAAAACCA | 102 |
| | S7-16F | GTGTCTGTGCCAGAAAGCTTGA | S7-16R | GAACCATGCAAAAGTGCCAATAT | 112 |
| RPS10 | S10-03F | CTACGGTTTTGTGTGGGTCACTT | S10-03R | CATCTGCAAGAAGGAGACGATTG | 102 |
| | S10-15F | GTTGGCCTGGAGTCGTGATTT | S10-15R | ATTCCAAGTGCACCATTTCCTT | 101 |
| | S10-17F | AATGGTGTTTAGGCCAACGTTAC | S10-17R | TTTGAACAGTGGTTTTTGTGCAT | 100 |
| RPS14 | S14-03F | GAATTCCAAACCCTTCTGCAAA | S14-03R | TTGCTTCATTTACTCCTCAAGACATT | 104 |
| | S14-05F | ACAACCAGCCCTCTACCTCTTTT | S14-05R | GGAAGACGCCGGCATTATT | 102 |
| | S14-06F | CGCCTCTACCTCGCCAAAC | S14-06R | GGGATCGGTGCTATTGTTATTCC | 102 |
| | S14-09F | GCCATCATGCCGAAACATACT | S14-09R | AACGCGCCACAGGAGAGA | 102 |
| | S14-13F | ATCAGGTGGAGCACAGGAAAAC | S14-13R | GCGAGGGAGCTGCTTGATT | 111 |
| | S14-15F | AGAAGTTTTAGTGAGGCAGAAATGAGA | S14-15R | TCCCCTGGCTATTAAATGAAACC | 102 |
| | S14-19F | GATGAATTGTCCTTTCCTCCATTC | S14-19R | TAGGCGGAAACCAAAAATGCT | 102 |
| RPS15 | S15-11F | CTCAGCTAATAAAGGCGCACATG | S15-11R | CCTCACACCACGAACCTGAAG | 108 |
| | S15-15F | GGTTGGAGAACATGGTGAGAACTA | S15-15R | CACATCCCTGGGCCACTCT | 108 |
| RPS17 | S17-03F | ACTGCTGTCGTGGCTCGATT | S17-03R | GATGACCTGTTCTTCTGGCCTTA | 121 |
| | S17-05F | GAAAACAGATACAAATGGCATGGT | S17-05R | TGCCTCCCACTTTTCCAGAGT | 114 |
| | S17-12F | CTATGTGTAGGAGGTCCCAGGATAG | S17-12R | CCACCTGGTACTGAGCACATGT | 102 |
| | S17-16F | TAGCGGAAGTTGTGTGCATTG | S17-16R | CAAGAACAGAAGCAGCCAAGAG | 102 |
| | S17-18F | TGGCTGAATCTGCCTGCTT | S17-18R | GCCTTGTATGTACCTGGAAATGG | 103 |
| | S17-20F | GGGCCCTTCACAAATGTTGA | S17-20R | GCAAAACTCTGTCCCTTTGAGAA | 101 |
| RPS19 | S19-24F | CCATCCCAAGAATGCACACA | S19-24R | CGCCGTAGCTGGTACTCATG | 120 |
| | S19-28F | GACACACCTGTTGAGTCCTCAGAGT | S19-28R | GCTTCTATTAACTGGAGCACACATCT | 114 |
| | S19-36F | CTCTTGAGGGTGGTCTGGAAAT | S19-36R | GTCTTTGCGGGTTCTTCCTCTAC | 102 |
| | S19-40F | GGAACGGTGTCAGGATTCAAG | S19-40R | AGCGGCTGTACACCAGAAATG | 101 |
| | S19-44F | CTGAGGTTGAGTGTCCCATTTCT | S19-44R | GCACCGGGCCTCTGTTATC | 104 |
| | S19-57F | CAGGGACACAGTGCTGAGAAACT | S19-57R | TGAGATGTCCCATTTTCACTATTGTT | 101 |
| | S19-58F | CATGATGTTAGCTCCGTTGCATA | S19-58R | ATTTTGGGAAGAGTGAAGCTTAGGT | 102 |
| | S19-62F | GCAACAGAGCGAGACTCCATTT | S19-62R | AGCACTTTTCGGCACTTACTTCA | 102 |
| | S19-65F | ACATTTCCCAGAGCTGACATGA | S19-65R | TCGGGACACCTAGACCTTGCT | 102 |
| RPS24 | S24-17F | CGACCACGTCTGGCTTAGAGT | S24-17R | CCTTCATGCCCAACCAAGTC | 101 |
| | S24-20F | ACAAGTAAGCATCATCACCTCGAA | S24-20R | TTTCCCTCACAGCTATCGTATGG | 105 |
| | S24-32F | GGGAAATGCTGTGTCCACATACT | S24-32R | CTGGTTTCATGGCTCCAGAGA | 105 |
| RPS26 | S26-03F | CGCAGCAGTCAGGGACATTT | S26-03R | AAGTTGGGCGAAGGCTTTAAG | 104 |
| | S26-05F | ATGGAGGCCGTCTAGTTTGGT | S26-05R | TGCCTACCCTGAACCTTGCT | 102 |
| RPS27A | S27A-09F | GCTGGAGTGCATTCGCTTGT | S27A-09R | CACGCCTGTAATCCCCACTAA | 102 |
| | S27A-12F | CAGGCTTGGTGTGCTGTGACT | S27A-12R | ACGTCCATCTTCCAGCTGCTT | 103 |
| | S27A-18F | GGGTTTTTCCTGTTTGGTATTTGA | S27A-18R | AAAGGCCAGCTTTGCAAGTG | 111 |
| | S27A-22F | TTACCATATTGCCAGTCTTTCCATT | S27A-22R | TTCATATGCATTTGCACAAACTGT | 106 |

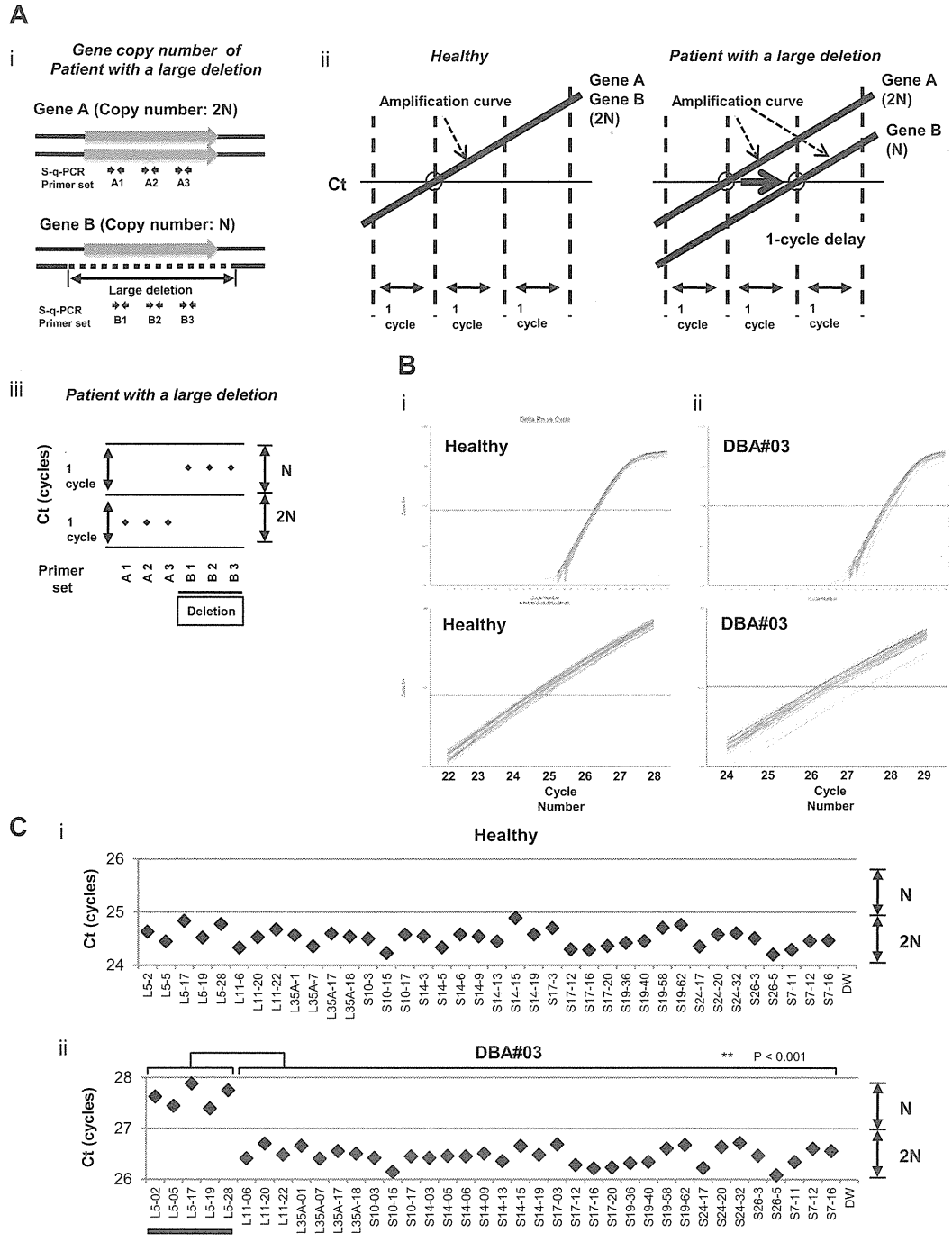


**Figure 1. s-q-PCR can determine a large gene deletion in DBA.** (A) Concept of the DBA s-q-PCR assay. The difference in gene copy number between a healthy sample and that with a large deletion is 2-fold (i). When all genomic s-q-PCR for genes of interest synchronously amplify DNA fragments, a 2-fold difference in the gene copy number is detected by a 1-cycle difference of the Ct scores of the s-q-PCR amplification curves (ii). Also shown is a dot plot of the Ct scores (iii). (B) Results of the amplification curves of s-q-PCR performed with a healthy person (i) and a DBA patient (patient 3; ii). The top panel shows the results of PCR cycles; the bottom panel is an extended graph of the PCR cycles at logarithmic amplification. (C) Graph showing Ct scores of s-q-PCR. If all specific primer sets for DBA genes show a 1-cycle delay relative to each other, this indicates a large deletion in the gene. Gene primer sets with a large deletion are underlined in the graph. $^{**}P < .001$.

small-for-gestational age (SGA), which suggests that this is a characteristic of DBA patients with a large gene deletion in Japan.

## Methods

### Patient samples

Genomic DNA was extracted using the GenElute Blood Genomic DNA Kit (Sigma-Aldrich) according to the manufacturer's protocol. Clinical manifestation of patients from a Japanese DBA genomic library are listed elsewhere or are as reported by Konno et al.[8] The study was approved by the institutional review board at the National Institute of Infectious Diseases and Hirosaki University.

### DBA gene copy number assay by s-q-PCR

For s-q-PCR, primers were designed using Primer Express Version 3.0 software (Applied Biosystems). Primers are listed in Tables 1 and 2. Genomic DNA in water was denatured at 95°C for 5 minutes and

immediately cooled on ice. The composition of the s-q-PCR mixture was as follows: 5 ng of denatured genomic DNA, 0.4mM forward and reverse primers, 1× SYBR Premix Ex Taq II (Takara), and 1× ROX reference dye II (Takara) in a total volume of 20 μL (all experiments were performed in duplicate). Thermal cycling was performed using the Applied Biosystems 7500 fast real-time PCR system. Briefly, the PCR mixture was denatured at 95°C for 30 seconds, followed by 35 cycles of 95°C for 5 seconds, 60°C for 34 seconds, and then dissociation curve measurement. Threshold cycle (Ct) scores were determined as the average of duplicate samples. The technical errors of Ct scores in the triplicate analysis were within 0.2 cycles (supplemental Figure 1, available on the *Blood* Web site; see the Supplemental Materials link at the top of the online article). The sensitivity and specificity of this method was evaluated with 15 healthy samples. Any false positive was not observed in all primer sets in all healthy samples (supplemental Figure 2). We performed direct sequencing of the s-q-PCR products. The results of the sequence analysis were searched for using BLAST to confirm uniqueness. Sequence data were obtained from GenBank (http://www.ncbi.nlm.nih.gov/gene/) and Ensemble Genome Browser (http://uswest.ensembl.org).

### Genomic PCR

Genomic PCR was performed using KOD FX (Toyobo) according to the manufacturer's step-down PCR protocol. Briefly, the PCR mixture contained 20 ng of genomic DNA, 0.4mM forward and reverse primers, 1mM dNTP, 1× KOD FX buffer, and 0.5 U KOD FX in a total volume of 25 μL in duplicate. Primers are given in supplemental Figure 3 and Table 2. PCR mixtures were denatured at 94°C for 2 minutes, followed by 4 cycles of 98°C for 10 seconds, 74°C for 12 minutes, followed by 4 cycles of 98°C for 10 seconds, 72°C for 12 minutes followed by 4 cycles of 98°C for 10 seconds, 70°C for 12 minutes, followed by 23 cycles of 98°C for 10 seconds and 68°C for 12 minutes. PCR products were loaded on 0.8% agarose gels and detected by LAS-3000 (Fujifilm).

### DNA sequencing analysis

The genomic PCR product was purified by the GenElute PCR clean-up kit (Sigma-Aldrich) according to the manufacturer's instructions. Direct sequencing was performed using the BigDye Version 3 sequencing kit. Sequences were read and analyzed using a 3120x genetic analyzer (Applied Biosystems).

### SNP array-based copy number analysis

SNP array experiments were performed according to the standard protocol of GeneChip Human Mapping 250K Nsp arrays (Affymetrix). Microarray data were analyzed for determination of the allelic-specific copy number using the CNAG program, as described previously.[14] All microarray data are available at the EGA database (www.ebi.ac.uk/ega) under accession number EGAS00000000105.

## Results

### Construction of a convenient method for RP gene copy number analysis based on s-q-PCR

We focused on the heterozygous large deletions in DBA-responsible gene. The difference in copy number of genes between a mutated DBA allele and the intact allele was 2-fold (N and 2N; Figure 1Ai). If each PCR can synchronously amplify DNA fragments when the template genomic DNA used is of normal karyotype, it is possible to conveniently detect a gene deletion with a 1-cycle delay in s-q-PCR analysis (Figure 1Aii-iii).

**Table 3. Summary of mutations and the mutation rate observed in Japanese DBA patients**

| Gene | Sequencing analysis |
|---|---|
| RPS19 | 10 |
| RPL5 | 6 |
| RPL11 | 3 |
| RPS17 | 1 |
| RPS10 | 1 |
| RPS26 | 1 |
| RPL35A | 0 |
| RPS24 | 0 |
| RPS14 | 0 |
| Mutations, n (%) | 22 (32.4%) |
| Total analyzed, N | 68 |

To apply this strategy for allelic analysis of DBA, we prepared primers for 16 target genes, *RPL5*, *RPL11*, *RPL35A*, *RPS10*, *RPS19*, *RPS26*, *RPS7*, *RPS17*, *RPS24*, *RPL9*, *RPL19*, *RPL26*, *RPL36*, *RPS14*, *RPS15*, and *RPS27A*, under conditions in which the Ct of s-q-PCR would occur within 1 cycle of that of the other primer sets (Tables 1 and 2). At the same time, we defined the criteria of a large deletion in our assay as follows. If multiple primer sets for one gene showed a 1-cycle delay from the other gene-specific primer set at the Ct score, we assumed that this represented a large deletion. As shown in Figure 1Bii and 1Cii, the specific primer sets for *RPL5* (L5-02, L5-05, L5-17, L5-19, and L5-28) detected a 1-cycle delay with respect to the mutated allele of patient 3. This assessment could be verified by simply confirming the difference of the cycles with the s-q-PCR amplification curves.

### Study of large gene deletions in a Japanese DBA genomic DNA library

Sixty-eight Japanese DBA patients were registered and blood genomic DNA was collected at Hirosaki University. All samples were first screened for mutations in *RPL5*, *L11*, *L35A*, *S10*, *S14*, *S17*, *S19*, and *S26* by sequencing. Among these patients, 32.4% (22 of 68) had specific DBA mutations (Table 3 and data not shown). We then screened for large gene deletions in 27 patients from the remaining 46 patients who did not possess mutations as determined by sequencing (Table 4).

When we performed the s-q-PCR DBA gene copy number assay, 7 of 27 samples displayed a 1-cycle delay of Ct scores: 1 patient had *RPL5* (patient 14), 1 had *RPL35A* (patient 71), 3 had *RPS17* (patients 3, 60, 62), and 2 had *RPS19* (patients 24 and 72; Figure 2 and Table 4). Among these patients, the large deletions in the *RPL5* and *RPS17* genes are the first reported cases of allelic deletions in DBA. From these results, we estimate that a sizable number of Japanese DBA patients have a large deletion.

Based on our findings, the rate of large deletions was approximately 25.9% (7 of 27) in a category of unspecified gene mutations. Such mutations have typically gone undetected by conventional sequence analysis. We could not find any additional gene deletions in the analyzed samples.

### Confirmation of the gene copy number for DBA genes by genome-wide SNP array

We performed genome-wide copy number analysis of the 27 DBA patients with a SNP array to confirm our s-q-PCR results. SNP array showed that patient 3 had a large deletion in

**Table 4. Characteristics of DBA patients tested**

| Patient no. | Age at diagnosis | Sex | Hb, g/dL | Large deletion by s-q-PCR | Large deletion by SNP array | Inheritance | Malformations | Response to first steroid therapy |
|---|---|---|---|---|---|---|---|---|
| **Patients with a large deletion in RP genes** | | | | | | | | |
| 3*† | 1 y | M | | RPL5 | RPL5 | Sporadic | Short stature, thumb anomalies | Response |
| 14* | 5 y | M | 5.5 | RPS17 | RPS17 | Sporadic | White spots, short stature | Response |
| 24*† | 1 mo | F | 5.5 | RPS19 | ND | Sporadic | Short stature, SGA | Response |
| 60*† | 2 mo | F | 2.4 | RPS17 | RPS17 | Sporadic | SGA | NT |
| 62*† | 1 mo | F | 6.2 | RPS17 | RPS17 | Sporadic | Small ASD, short stature, SGA | Response |
| 71 | 0 y | M | 5.3 | RPL35A | RPL35A | Sporadic | Thumb anomalies, synostosis of radius and ulna, Cohelia Lange-like face, cleft palate, underdescended testis, short stature, cerebellar hypoplasia, fetal hydrops | NT |
| 72† | 0 y | M | 2 | RPS19 | RPS19 | Sporadic | Thumb anomalies, flat thenar, testicular hypoplasia, fetal hydrops, short stature, learning disability | No |
| **Patients without a large deletion in RP genes** | | | | | | | | |
| 5* | 1 y | F | 3.1 | ND | ND | Sporadic | ND | Response |
| 15* | 1 mo | F | 1.6 | ND | ND | Sporadic | ND | Response |
| 21* | 1 y | F | 2.6 | ND | ND | Sporadic | ND | Response |
| 26* | 1 y 1 mo | F | 8 | ND | ND | Sporadic | Congenital hip dislocation, spastic quadriplegia, hypertelorism, nystagmus, short stature, learning disability | Response |
| 33* | 2 mo | F | 1.3 | ND | ND | Sporadic | ND | Response |
| 36* | 0 y | M | 8.2 | ND | ND | Familial | ND | Response |
| 37* | 4 y | M | 6.1 | ND | ND | Sporadic | Hypospadias, underdescended testis, SGA | NT |
| 45* | 5 d | M | 5.1 | ND | ND | Sporadic | Short stature, microcephaly, mental retardation, hypogammaglobulinemia | Poor |
| 50* | 2 m | F | 3.4 | ND | ND | Familial | ND | Response |
| 61* | 9 m | M | 4 | ND | ND | Sporadic | ND | Response |
| 63* | 0 y | M | 6.8 | ND | ND | Sporadic | Micrognathia, hypertelorism, short stature | Response |
| 68 | 1 y 4 mo | M | 5.9 | ND | ND | Sporadic | ND | NT (CR) |
| 69 | 1 y | M | 9.3 | ND | ND | Sporadic | ND | Response |
| 76 | 0 y | M | 4 | ND | ND | Sporadic | ND | Response |
| 77 | 0 y | M | 7.8 | ND | ND | Familial | Short stature | No |
| 83 | 9 mo | F | 3 | ND | ND | Sporadic | ND | NT |
| 90 | 10 mo | M | 9 | ND | ND | Sporadic | ND | No |
| 91 | 0 y | F | 3.8 | ND | ND | Sporadic | ND | Response |
| 92 | 2 mo | M | 3.7 | ND | ND | Sporadic | ASD, PFO, melanosis, underdescended testis, SGA, short stature | Response |
| 93 | 11 mo | M | 2.2 | ND | ND | Sporadic | White spots, senile face, corneal opacity, underdescended testis, syndactyly, ectrodactyly, flexion contracture, extension contracture | Response |

ND indicates not detected; NT, not tested; CR, complete remission; ASD, atrial septal defect; and PFO, persistent foramen ovale.

*Status data of Japanese probands 3 to 63 is from a report by Konno et al.[8]

†Large deletions of the parents of 5 DBA patients (3, 24, 60, 62, and 72) were analyzed by s-q-PCR, but there were no deletions in DBA genes in any of the 5 pairs of parents.

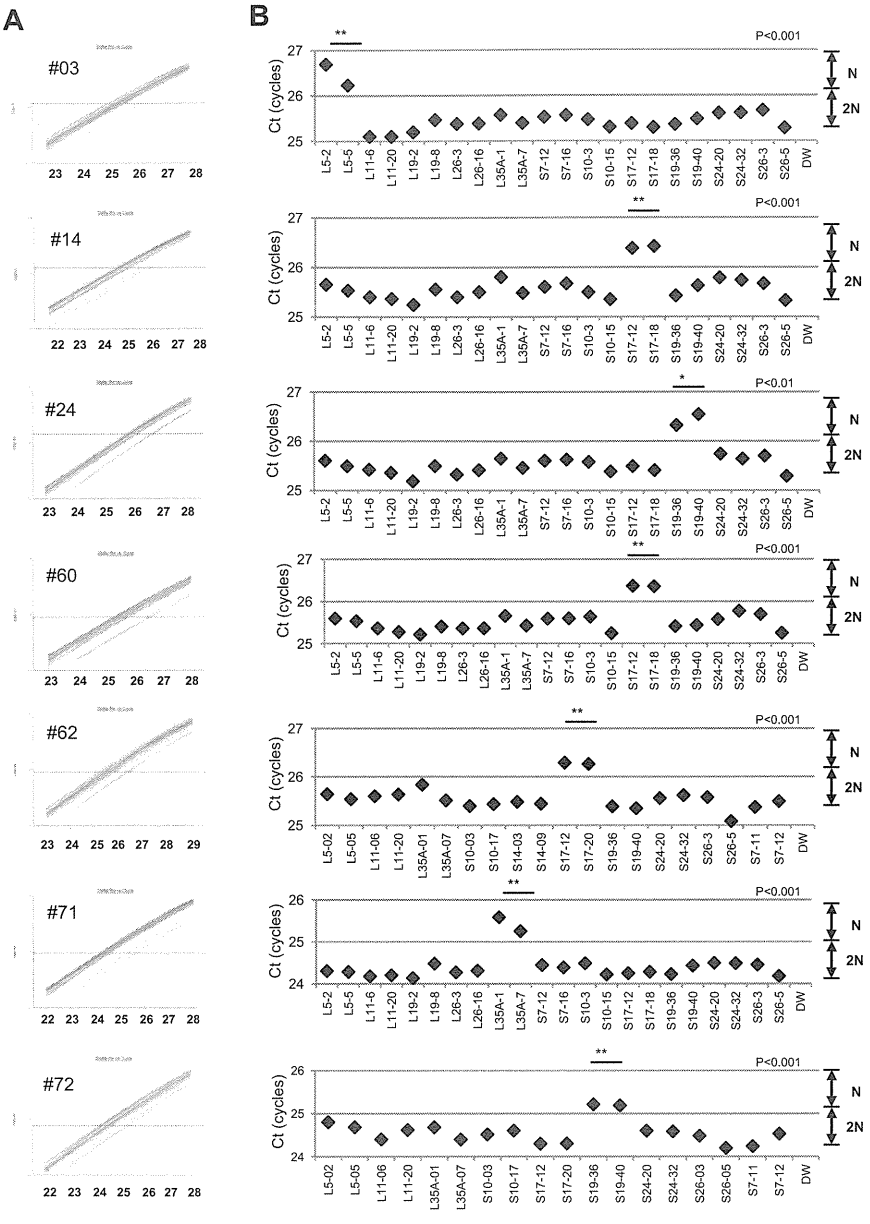


**Figure 2. Detection of 7 mutations with a large deletion in DBA patients.** Genomic DNA of 27 Japanese DBA patients with unknown mutations were subjected to the DBA gene copy number assay. (A) Amplification curve of s-q-PCR of a mutation with a large deletion. The deleted gene can be easily distinguished. (B) Ct score (cycles) of representative s-q-PCR with DBA genomic s-q-PCR primers. Results of the 2 gene-specific primer pairs indicated in the graph are representative of at least 2 sets for each gene-specific primer (carried out in the same run). $^{**}P < .001$; $^{*}P < .01$

chromosome 1 (ch1) spanning 858 kb (Figure 3A); patient 71 had a large deletion in ch3 spanning 786 kb (Figure 3B); patients 14, 60, and 62 had a large deletion in ch15 spanning 270 kb, 260 kb, and 330 kb, respectively (Figure 3C); and patient 72 had a large deletion in ch19 spanning 824 kb (Figure 3D). However, there were no deletions detected in ch19 in patient 24 (Figure 3D). Genes estimated to reside within a large deletion are listed in supplemental Table 1. Consistent with these s-q-PCR results, 6 of 7 large deletions were detected and confirmed as deleted regions, and these large deletions contained *RPL5*, *RPL35A*, *RPS17*, and *RPS19* (Table 4 and supplemental Table 1). Other large deletions in RP genes were not detected by this analysis. From these results, we conclude that the synchronized multiple PCR amplification method has a detection sensitivity comparable to that of SNP arrays.

### Detailed examination of a patient with intragenic deletion in the RPS19 allele (patient 24)

Interestingly, for patient 24, in whom we could not detect a large deletion by SNP array at s-q-PCR gene copy number analysis, 2 primer sets for *RPS19* showed a 1-cycle delay (RPS19-36 and RPS19-40), but 2 other primer pairs (RPS19-58 and RPS19-62) did not show this delay (Figure 4A). We attempted to determine the deleted region in detail by testing more primer sets on *RPS19*. We tested a total of 9 primer sets for *RPS19* (Figure 4B) and examined the gene copy numbers. Surprisingly, 4 primer sets (S19-24, S19-36, S19-40, and S19-44) for intron 3 of *RPS19* indicated a 1-cycle delay, but the other primers for *RPS19* located on the 5′untranslated region (5′UTR), intron 3, or 3′UTR did not show this delay (S19-57, S19-58, S19-28, S19-62, and S19-65; Figure 4B-C). These results suggest that the intragenic deletion occurred in the *RPS19* allele. To confirm this deleted region precisely, we performed genomic PCR on *RPS19*, amplifying a region from the 5′UTR to intron 3 (Figure

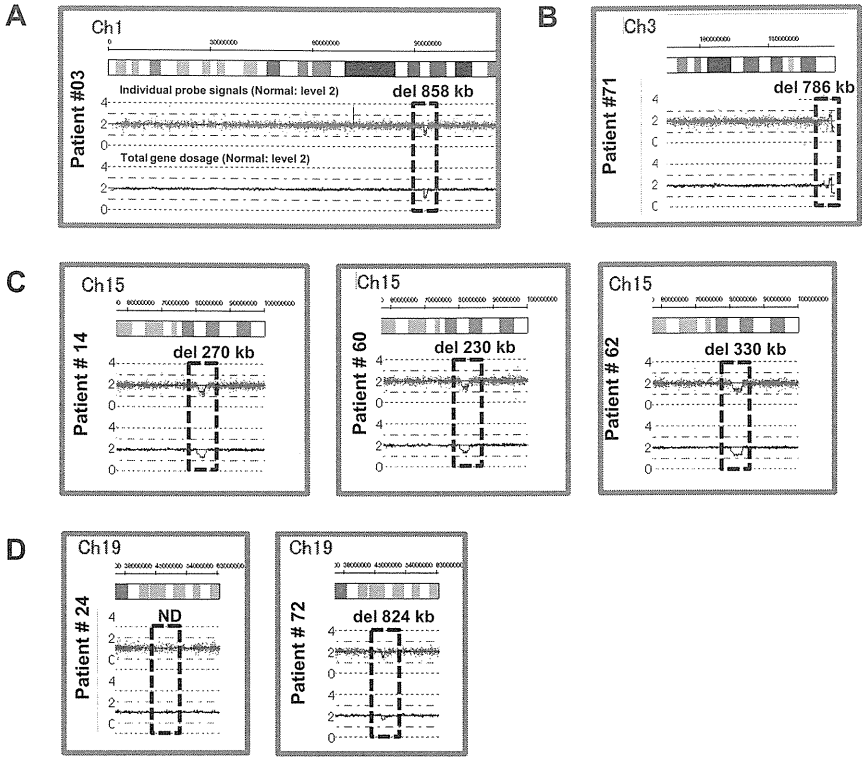


**Figure 3. Results of SNP genomic microarray (SNP-chip) analysis.** Genomic DNA of 27 Japanese DBA patients with unknown mutations was examined using a SNP array. Six patients had large deletions in their chromosome (ch), which included one DBA-responsible gene. Patient 3 has a large deletion in ch1 (A), patient 71 has a deletion in ch3 (B), patients 14, 60, and 62 have deletions in ch15 (C), and patient 72 has a deletion in ch19 (D).

4B). In patient 24, we observed an abnormally sized PCR product at a low molecular weight by agarose gel electrophoresis (Figure 4D). We did not detect a wild-type PCR product from the genomic PCR. This finding is probably because PCR tends to amplify smaller molecules more easily. However, we did detect a PCR fragment at the correct size using primers located in the supposedly deleted region. These bands were thought to be from the products of a wild-type allele. Sequencing of the mutant band revealed that intragenic recombination occurred at a homologous region of 27 nucleotides, from −1400 to −1374 in the 5′ region, to +5758 and +5784 in intron 3, which resulted in the loss of 7157 base pairs in the *RPS19* gene (Figure 4E). The deleted region contains exons 1, 2, and 3, and therefore the correct *RPS19* mRNA could not be transcribed.

### Genotype-phenotype analysis and DBA mutations in Japan

Patients with a large deletion in DBA genes had common phenotypes (Table 4). Malformation with growth retardation (GR), including short stature or SGA, were observed in all 7 patients. In patients who had a mutation found by sequencing, half had GR (11 of 22; status data of DBA patients with mutations found by sequencing are not shown). GR may be a distinct phenotypic feature of large deletion mutations in Japanese DBA patients. Familial mutations were analyzed for parents for 5 DBA patients with a large deletion (patients 3, 24, 60, 62, and 72) by s-q-PCR. There are no large deletions in all 5 pairs of parents in DBA-responsible genes. Four of the 7 patients responded to steroid therapy. We have not observed significant phenotypic differences between patients with extensive deletions and other patients with regard to blood counts, responsiveness to treatment, or other malformations.

## Discussion

Many studies have reported RP genes to be responsible for DBA. However, mutations have not been determined for approximately half of DBA patients analyzed. There are 2 possible reasons for this finding. One possibility is that patients have other genes responsible for DBA, and the other is that patients have a complicated set of mutations in RP genes that are difficult to detect. In the present study, we focused on the latter possibility because we have found fewer Japanese DBA patients with RP gene mutations (32.4%) compared with another cohort study of 117 DBA patients and 9 RP genes (approximately 52.9%).[4] With our newly developed method, we identified 7 new mutations with a large deletion in *RPL5*, *RPL35A*, *RPS17*, and *RPS19*.

The frequency of a large deletion was approximately 25.9% (7 of 27) in our group of patients who were not found to have mutations by genomic sequencing. Therefore, total RP gene mutations were confirmed in 42.6% of these Japanese patients (Table 5). Interestingly, mutations in *RPS17* have been observed at a high rate (5.9%) in Japan relative to that in other countries (1%).[5,15,16] Although the percentage of DBA mutations differs among different ethnic groups,[8,17-19] a certain portion of large deletions in DBA-responsible genes are likely to be determined in other countries by new strategies.

In the present study, we analyzed patient data to determine genotype-phenotype relations. To date, large deletions have been reported with RPS19 and RPL35A in DBA patients.[3,6,13] *RPS19* large deletions/translocations have been reported in 12 patients, and *RPL35A* large deletions have been reported in 2 patients.[19] GR in patients with a large deletion has been observed previously with *RPS19* translocations,[3,19-21] but it was not found in 2 patients with *RPL35A* deletion.[6] Interestingly, all of our patients with a large deletion had a phenotype

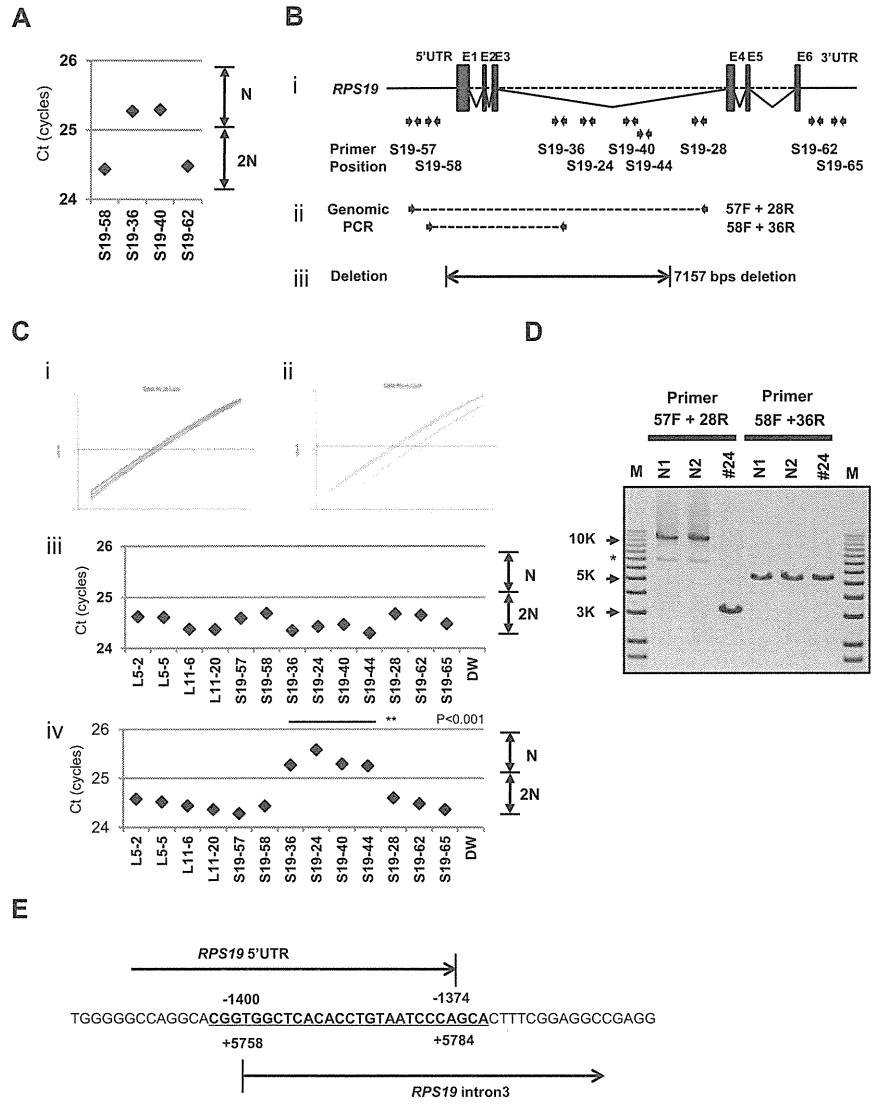


**Figure 4. Result of s-q-PCR gene copy number assay for patient 24.** (A) Results of s-q-PCR gene copy number assay for *RPS19* with 4 primer sets. (Bi) The *RPS19* gene copy number was analyzed with 9 specific primer sets for *RPS19* that span from the 5′UTR to the 3′UTR. (ii) Primer positions of genomic PCR for *RPS19*. (iii) Region determined to be an intragenic deletion in *RPS19*. (C) Results of gene copy number assay for *RPS19* show a healthy person (i,iii) and a DBA patient (ii,iv), and Ct results are shown (iii-iv). Patient 24 showed a "1-cycle delay" with primers located in the intron 3 region, but other primer sets were normal. (D) Results of genomic PCR amplification visualized by agarose gel electrophoresis to determine the region of deletion. N1 and N2 are healthy samples. *Nonspecific band. (E) Results from the genomic sequence of the 3-kb DNA band from genomic PCR on patient 24 showing an intragenic recombination from −1400 to 5784 (7157 nt) in *RPS19*. $^{**}P < .001$.

of GR, including short stature and SGA, which suggests that this is a characteristic of DBA with a large gene deletion in Japan. Our study results suggest the possibility that GR is associated with extensive deletion in Japanese patients. Although further case studies will be needed to confirm this possibility, screening of DBA samples using our newly developed method will help to advance our understanding of the broader implications of the mutations and the correlation with the DBA genotype-phenotype.

**Table 5. Total mutations in Japanese DBA patients, including large gene deletions**

| Gene | Mutation rate |
|---|---|
| RPS19 | 12(17.6%) |
| RPL5 | 7(10.3%) |
| RPL11 | 3 (4.4%) |
| RPS17 | 4 (5.9%) |
| RPS10 | 1 (1.5%) |
| RPS26 | 1 (1.5%) |
| RPL35A | 1 (1.5%) |
| RPS24 | 0 |
| RPS14 | 0 |
| Mutations, n (%) | 29(42.6%) |
| Total analyzed, N | 68 |

Copy number variation analysis of DBA has been performed by linkage analysis, and the *RPS19* gene was first identified as a DBA-susceptibility gene. Comparative genomic hybridization array technology has also been used to detect DBA mutations in *RPL35A*, and multiplex ligation-dependent probe amplification has been used for *RPS19* gene deletion analysis.[3,6,13,22] However, these analyzing systems have problems in mutation screening. Linkage analysis is not a convenient tool to screen for multiple genetic mutations, such as those in DBA, because it requires a high level of proficiency. Although comparative genomic hybridization technology is a powerful tool with which to analyze copy number comprehensively, this method requires highly specialized equipment and analyzing software, which limits accessibility for researchers. Whereas quantitative PCR–based methods for copy number variation analysis are commercially available (TaqMan), they require a standard curve for each primer set, which limits the number of genes that can be loaded on a PCR plate. To address this issue, a new method of analysis is needed. By stringent selection of PCR primers, the s-q-PCR method enables analysis of many DBA genes in 1 PCR plate and the ability to immediately distinguish a large deletion using the s-q-PCR amplification curve. In our study, 6 of 7 large deletions in the RP gene detected by s-q-PCR were confirmed by SNP arrays (Figure 3). Interestingly, we detected

1 large intragenic deletion in *RPS19*, which was not detected by the SNP array. This agreement between detection results suggests that the s-q-PCR copy number assay could be useful for detecting large RP gene deletions.

In the present study, 7 DBA patients carried a large deletion in the RP genes. This type of mutation could be underrepresented by sequencing analysis, although in the future, genome sequencing might provide a universal platform for mutation and deletion detection. We propose that gene copy number analysis for known DBA genes, in addition to direct sequencing, should be performed to search for a novel responsible gene for DBA. Although at present, it may be difficult to observe copy numbers on all 80 ribosomal protein genes in one s-q-PCR assay, our method allows execution of gene copy number assays for several target genes in 1 plate. Because our method is quick, easy, and low cost, it could become a conventional tool for detecting DBA mutations.

## Acknowledgments

The authors thank Momoka Tsuruhara, Kumiko Araki, and Keiko Furuhata for their expert assistance.

This work was partially supported by grants-in-aid for scientific research from the Ministry of Education, Culture, Sports, Science and Technology of Japan, and by Health and Labor Sciences research grants (Research on Intractable Diseases) from the Ministry of Health, Labor and Welfare of Japan.

## Authorship

Contribution: M.K. designed and performed the research, analyzed the data, and wrote the manuscript; A.S-O. and S. Ogawa performed the SNP array analysis; T.M., M.T., and M.O designed the study; T.T, K. Terui, and R.W. analyzed the mutations and status data; H.K., S. Ohga, A.O., S.K., T.K., K.G., K.K., T.M., and N.M. analyzed the status data; A.M., H.M., K. Takizawa, T.M., and K.Y., performed the research and analyzed the data; E.I. and I.H. designed the study and analyzed the data; and all authors wrote the manuscript.

Conflict-of-interest disclosure: The authors declare no competing financial interests.

Correspondence: Isao Hamaguchi, MD, PhD, Department of Safety Research on Blood and Biological Products, National Institute of Infectious Diseases, 4-7-1, Gakuen, Musashimurayama, Tokyo 208-0011, Japan; e-mail: 130hama@nih.go.jp; or Etsuro Ito, MD, PhD, Department of Pediatrics, Hirosaki University Graduate School of Medicine, 5 Zaifucho, Hirosaki, Aomori 036-8562, Japan; e-mail: eturou@cc.hirosaki-u.ac.jp.

## References

1. Hamaguchi I, Flygare J, Nishiura H, et al. Proliferation deficiency of multipotent hematopoietic progenitors in ribosomal protein S19 (RPS19)-deficient diamond-Blackfan anemia improves following RPS19 gene transfer. *Mol Ther.* 2003;7(5 pt 1):613-622.
2. Vlachos A, Ball S, Dahl N, et al. Diagnosing and treating Diamond Blackfan anaemia: results of an international clinical consensus conference. *Br J Haematol.* 2008;142(6):859-876.
3. Draptchinskaia N, Gustavsson P, Andersson B, et al. The gene encoding ribosomal protein S19 is mutated in Diamond-Blackfan anaemia. *Nat Genet.* 1999;21(2):169-175.
4. Doherty L, Sheen MR, Vlachos A, et al. Ribosomal protein genes RPS10 and RPS26 are commonly mutated in Diamond-Blackfan anemia. *Am J Hum Genet.* 2010;86(2):222-228.
5. Gazda HT, Sheen MR, Vlachos A, et al. Ribosomal protein L5 and L11 mutations are associated with cleft palate and abnormal thumbs in Diamond-Blackfan anemia patients. *Am J Hum Genet.* 2008;83(6):769-780.
6. Farrar JE, Nater M, Caywood E, et al. Abnormalities of the large ribosomal subunit protein, Rpl35a, in Diamond-Blackfan anemia. *Blood.* 2008;112(5):1582-1592.
7. Gazda HT, Grabowska A, Merida-Long LB, et al. Ribosomal protein S24 gene is mutated in Diamond-Blackfan anemia. *Am J Hum Genet.* 2006;79(6):1110-1118.
8. Konno Y, Toki T, Tandai S, et al. Mutations in the ribosomal protein genes in Japanese patients with Diamond-Blackfan anemia. *Haematologica.* 2010;95(8):1293-1299.
9. Robledo S, Idol RA, Crimmins DL, Ladenson JH, Mason PJ, Bessler M. The role of human ribosomal proteins in the maturation of rRNA and ribosome production. *RNA.* 2008;14(9):1918-1929.
10. Léger-Silvestre I, Caffrey JM, Dawaliby R, et al. Specific Role for Yeast Homologs of the Diamond Blackfan Anemia-associated Rps19 Protein in Ribosome Synthesis. *J Biol Chem.* 2005;280(46):38177-38185.
11. Choesmel V, Fribourg S, Aguissa-Toure AH, et al. Mutation of ribosomal protein RPS24 in Diamond-Blackfan anemia results in a ribosome biogenesis disorder. *Hum Mol Genet.* 2008;17(9):1253-1263.
12. Flygare J, Aspesi A, Bailey JC, et al. Human RPS19, the gene mutated in Diamond-Blackfan anemia, encodes a ribosomal protein required for the maturation of 40S ribosomal subunits. *Blood.* 2007;109(3):980-986.
13. Quarello P, Garelli E, Brusco A, et al. Multiplex ligation-dependent probe amplification enhances molecular diagnosis of Diamond-Blackfan anemia due to RPS19 deficiency. *Haematologica.* 2008;93(11):1748-1750.
14. Yamamoto G, Nannya Y, Kato M, et al. Highly sensitive method for genomewide detection of allelic composition in nonpaired, primary tumor specimens by use of affymetrix single-nucleotide-polymorphism genotyping microarrays. *Am J Hum Genet.* 2007;81(1):114-126.
15. Song MJ, Yoo EH, Lee KO, et al. A novel initiation codon mutation in the ribosomal protein S17 gene (RPS17) in a patient with Diamond-Blackfan anemia. *Pediatr Blood Cancer.* 2010;54(4):629-631.
16. Cmejla R, Cmejlova J, Handrkova H, Petrak J, Pospisilova D. Ribosomal protein S17 gene (RPS17) is mutated in Diamond-Blackfan anemia. *Hum Mutat.* 2007;28(12):1178-1182.
17. Cmejla R, Cmejlova J, Handrkova H, et al. Identification of mutations in the ribosomal protein L5 (RPL5) and ribosomal protein L11 (RPL11) genes in Czech patients with Diamond-Blackfan anemia. *Hum Mutat.* 2009;30(3):321-327.
18. Quarello P, Garelli E, Carando A, et al. Diamond-Blackfan anemia: genotype-phenotype correlations in Italian patients with RPL5 and RPL11 mutations. *Haematologica.* 2010;95(2):206-213.
19. Boria I, Garelli E, Gazda HT, et al. The ribosomal basis of Diamond-Blackfan Anemia: mutation and database update. *Hum Mutat.* 2010;31(12):1269-1279.
20. Campagnoli MF, Garelli E, Quarello P, et al. Molecular basis of Diamond-Blackfan anemia: new findings from the Italian registry and a review of the literature. *Haematologica.* 2004;89(4):480-489.
21. Willig TN, Draptchinskaia N, Dianzani I, et al. Mutations in ribosomal protein S19 gene and diamond blackfan anemia: wide variations in phenotypic expression. *Blood.* 1999;94(12):4294-4306.
22. Gustavsson P, Garelli E, Draptchinskaia N, et al. Identification of microdeletions spanning the Diamond-Blackfan anemia locus on 19q13 and evidence for genetic heterogeneity. *Am J Hum Genet.* 1998;63(5):1388-1395.

Pediatr Blood Cancer 2012;59:530–535

# Mutations Profile of Polycythemia Vera and Essential Thrombocythemia Among Japanese Children

Olfat Ismael, MD,[1] Akira Shimada, MD, PhD,[1] Asahito Hama, MD, PhD,[1] Hiroshi Sakaguchi, MD,[1] Sayoko Doisaki, MD,[1] Hideki Muramatsu, MD, PhD,[1] Nao Yoshida, MD, PhD,[2] Masafumi Ito, MD, PhD,[3] Yoshiyuki Takahashi, MD, PhD,[1] Naohiro Akita, MD, PhD,[4] Shosuke Sunami, MD, PhD,[4] Yoshitoshi Ohtsuka, MD, PhD,[5] Youji Asada, MD, PhD,[6] Hiroyuki Fujisaki, MD, PhD,[7] and Seiji Kojima, MD, PhD[1]*

***Background.*** Acquired somatic mutations of *JAK2* have been reported to play a pivotal role in the pathogenesis of *BCR-ABL1*-negative myeloproliferative neoplasm (MPN). However, the molecular characteristics of childhood MPN remain to be elucidated. ***Patient and Methods.*** We investigated a group of pediatric patients diagnosed either with essential thrombocythemia (ET; N = 9) or polycythemia vera (PV; N = 4) according to WHO criteria (median age = 10 years; range 1.5–15 years) in whom direct sequencing was performed for the existence of genetic alterations in *JAK2, MPL, TET2, ASXL1, CBL, IDH1,* and *IDH2*. More sensitive allele specific polymerase chain reaction was used for $JAK2^{V617F}$ genotyping. ***Results.*** We found three patients harbor $JAK2^{V617F}$ mutation (2/9 ET and 1/4 PV). Bone marrow examination showed small and large megakaryocytes with dysplastic features in $JAK2^{V617F}$-positive ET patients compared to those without $JAK2^{V617F}$. We identified a previously unrecognized missense mutation at codon 1230 in exon 12 of *ASXL1* gene in ET and PV patients (1/9 ET and 1/4 PV). Otherwise, no genetic alterations could be detected in *JAK2* exon 12, *MPL, TET2, CBL, IDH1,* and *IDH2* in all ET and PV patients. ***Conclusion.*** Although *JAK2* mutations in childhood ET and PV are not as frequent as reported in adult patients, *JAK2* is the most frequently mutated gene in childhood MPN known so far. Owing to the presence of childhood MPN without any genetic alterations in *JAK2, MPL, TET2, ASXL1, CBL, IDH1,* and *IDH2*, new biological markers have to be found. Pediatr Blood Cancer 2012;59:530–535. © 2011 Wiley Periodicals, Inc.

**Key words:** *ASXL1*; essential thrombocythemia; *JAK2*; mutation; polycythemia vera

## INTRODUCTION

Polycythemia vera (PV), essential thrombocythemia (ET), and myelofibrosis (MF) are stem cell derived clonal myeloproliferative neoplasms (MPN) that result in overproduction of mature myeloid cells. Although they are recognized as a distinct clinicopathological entity, they share cardinal biological features that differentiate them from other myeloid malignancies [1]. In patients with PV there is a prevalent increase of the red cell line often associated with high granulocyte and platelet numbers, while ET is associated with an isolated elevated platelet count [2].

Genetic studies have identified that $JAK2^{V617F}$ is the most frequent mutation in BCR-ABL-negative MPN [3–8]. Analysis of *JAK2* alterations is generally accepted to be an essential component in the diagnostic criteria for PV and ET [9]. Furthermore, gain-of-function mutations in *JAK2* exon 12 and in thrombopoietin receptor (*MPL*) are observed in some patients with $JAK2^{V617F}$-negative MPN, suggesting constitutive activation of *JAK2* signaling is important in the pathogenesis of adult PV, ET, and MF [10].

Ten-eleven-translocation 2 (*TET2*) mutations were reported in various adult hematopoietic disorders including MPN [11]. It was mentioned that loss-of-function *TET2* mutations may precede or follow the acquisition of $JAK2^{V617F}$ mutation which result in accelerated cellular proliferation and contribute to the aggressive behavior of MPN [12]. Recently, mutations in Additional sex comb-like 1 (*ASXL1*), casitas B-Lineage lymphoma (*CBL*), isocitrate dehydrogenase 1 (*IDH1*) and the homologous gene *IDH2* have been described in adult MPN [13–15]. So far, the occurrence of these mutations has not been reported in childhood MPN.

Although pediatric and adult MPN exhibit similar hematologic findings, MPN in childhood is quite rare disease [3,16]. Thus, application of any diagnostic criteria developed for adult MPN would be helpful to know the biological difference between childhood and adulthood MPN [17]. In the light of this background and to better understand the molecular pathogenesis of MPN in childhood, we investigated the genetic alterations of *JAK2* ($^{V617F}$ and exon 12), *TET2* (all exons), *ASXL1* (exon 12), *CBL* (exons 7–9), *IDH1* and *IDH2* (exon 4) among PV and ET pediatric patients. Also we evaluated the occurrence of *MPL* (exon 10) mutations in *V617F*-negative ET patients.

## PATIENTS AND METHODS

### Recruitment of PV and ET Patients and Healthy Candidates

We evaluated 13 Japanese children with a diagnosis of ET (n = 9) and PV (n = 4) consecutively observed between 2005 and 2010. All patients were diagnosed in accordance to WHO criteria [18]. None of the patients had a positive family history for ET or PV. Peripheral blood and/or bone marrow samples were collected and mononuclear cell fraction was isolated and subjected to molecular analysis. Thirty healthy volunteers were

[1]Department of Pediatrics, Nagoya University Graduate School of Medicine, Nagoya, Aichi, Japan; [2]Department of Pediatrics, Japanese Red Cross Nagoya First Hospital, Nagoya, Aichi, Japan; [3]Department of Pathology, Japanese Red Cross Nagoya First Hospital, Nagoya, Aichi, Japan; [4]Department of Pediatric Hematology/Oncology, Narita Red Cross Hospital, Narita, Chiba, Japan; [5]Department of Pediatrics, Hyogo College of Medicine, Nishinomiya, Hyogo, Japan; [6]Department of Pediatrics, Iwaki-kyouritsu General Hospital, Iwaki, Japan; [7]Department of Pediatric Hematology/Oncology, Osaka City General Hospital, Osaka, Japan

Conflict of interest: Nothing to declare.

*Correspondence to: Seiji Kojima, MD, PhD, 65 Tsurumai-cho, Showaku, Nagoya, Aichi, 466-8550 Japan.
E-mail: kojimas@med.nagoya-u.ac.jp

Received 14 August 2011; Accepted 30 September 2011


DOI 10.1002/pbc.23409
Published online 21 November 2011 in Wiley Online Library (wileyonlinelibrary.com).

recruited as controls in this study. Throughout the research, we adhered to the Japanese ethical guidelines for epidemiologic studies; and the study protocol was approved by the Institutional Review Boards of Nagoya University Graduate School of Medicine. Informed consent was obtained from the guardians of the patients following institutional guidelines.

## DNA Isolation

Mononuclear cells were separated from aspirated bone marrow and/or peripheral blood samples using a Ficoll gradient. Genomic DNA was isolated using the QIAmp DNA blood mini kit (Qiagen, Hilden, Germany) according to the manufacturer's protocol.

## Sequence Analysis

Somatic mutations in exons 12, 14 of *JAK2* [3], exon 10 of *MPL* [19], all exons of *TET2* [11], exon 12 of *ASXL1* [20], exons 7–9 of *CBL* [14], exon 4 of *IDH1* and *IDH2* [15], were searched by sequencing analysis after polymerase chain reaction (PCR) amplification of genomic DNA. PCR amplification were done in a total volume of 25 μl PCR mix containing at least 50 ng template DNA, using quick Taq PCR™ HS Dye mix (Qiagen) under the following conditions: 94°C, 2 minutes (first denaturing step); 94°C, 30 seconds; 65°C, 30 seconds; 68°C, 30 seconds to 1 minute depending on PCR product length for 35 cycles; 68°C, 7 minutes (last extension step). PCR products were purified from the reaction mixture using the QIA quick PCR purification kit (Qiagen) and directly sequenced on a DNA sequencer (ABI PRISM 3100 Genetic Analyzer Applied Biosystems, Life Technologies Japan, Tokyo) using a Big Dye terminator cycle sequencing kit (Applied Biosystems).

## Allele-Specific PCR

In combination with sequence analysis to screen $JAK2^{V617F}$ mutation efficiently, we carried out allele-specific PCR analysis according to the procedures described elsewhere [3].

# RESULTS

## Clinical and Hematological Characteristics of ET and PV Patients

Nine ET patients (five females, four males) with a median age at onset of 11.5 years (range 1.5–15 years) were included. The data of these patients are summarized in Table I. The median white blood cell counts, hemoglobin levels, and platelet counts were $10.4 \times 10^9$/L (range 5.8–19.4 $\times$ $10^9$/L), 13.3 g/dl (range 11.7–15.2 g/dl), and $1.827 \times 10^9$/L (range 923–2.900 $\times$ $10^9$/L), respectively. No clinical or laboratory evidence of chronic infections could be detected in this group of patients. Histopathological examination of bone marrow showed an elevated number of megakaryocytes in all ET patients. Interestingly, in two ET patients with $JAK2^{V617F}$ mutation (case no. 7 and case no. 11) small size and dysplastic changes of megakaryocytes (multinucleated and binucleated cells) were found, these findings raise the possibilities that $JAK2^{V617F}$ may be responsible for the distinct pathological features of bone marrow seen in those ET patients (Fig. 1). Four PV patients (two females and two males) were also evaluated in this cohort. The age at diagnosis for PV patients ranged from

**TABLE I. Clinical Characteristics of 13 Pediatric Cases With Essential Thrombocythemia and Polycythemia Vera**

| Id | S/A (Y) | D | Sp | WBC ($\times 10^9$/L) | RBCs ($\times 10^{12}$/L) | Hb (g/dl) | Ht (%) | Plt ($\times 10^9$/L) | Ph ch | *JAK2 V617F* | *JAK2* exon 12 | *MPL* exon 10 | *TET2* | *ASXL1* exon 12[a] | *CBL* | *IDH1/ IDH2* | Therapy | FUP (Y) |
|---|---|---|---|---|---|---|---|---|---|---|---|---|---|---|---|---|---|---|
| 1 | F/12 | ET | − | 10.3 | 4.2 | 11.7 | 35.3 | 238.4 | − | − | − | − | − | − | − | −/− | Aspirin | 20 |
| 2 | M/12 | ET | − | 10.4 | 4.2 | 11.8 | 35.2 | 290.0 | − | − | − | − | − | − | − | −/− | Aspirin | 15 |
| 3 | M/12 | ET | − | 9.4 | 5 | 13.3 | 41.4 | 230.6 | − | − | − | − | − | − | − | −/− | Aspirin | 13 |
| 4 | M/5 | ET | − | 19.4 | 4.9 | 12.5 | 38.2 | 182.7 | − | − | − | − | − | + | − | −/− | Aspirin | 3 |
| 5 | F/7 | PV | − | 14.6 | 5.7 | 15.8 | 46.2 | 529 | − | − | − | nt | − | + | − | −/− | — | 5 |
| 6 | M/15 | ET | + | 5.8 | 5.1 | 14 | 42.5 | 923 | − | − | − | − | − | − | − | −/− | Aspirin | 5 |
| 7 | F/8 | ET | + | 18.9 | 5.2 | 15.2 | 43.6 | 956 | − | + | − | − | − | − | − | −/− | — | 10 |
| 8 | M/15 | PV | − | 6.6 | 5.9 | 19 | 54.6 | 248 | − | − | − | nt | − | − | − | −/− | — | 4 |
| 9 | F/14 | PV | + | 16.5 | 8.5 | 16.9 | 57.8 | 114 | − | − | − | nt | − | − | − | −/− | Phlebotomy | 5 |
| 10 | M/14 | PV | − | 19.2 | 9.8 | 21.8 | 71.5 | 210 | − | + | − | nt | − | − | − | −/− | — | 7 |
| 11 | F/1.5 | ET | − | 15.2 | 5.8 | 13.5 | 40.7 | 106.4 | − | + | − | − | − | − | − | −/− | — | 1 |
| 12 | M/11 | ET | − | 10.4 | 5 | 12.9 | 39.9 | 144.8 | − | − | − | − | − | − | − | −/− | — | 1 |
| 13 | F/9 | ET | − | 14.1 | 5.1 | 13.8 | 41.9 | 245.5 | − | − | − | − | − | − | − | −/− | Aspirin | 1 |

Id, patient's number; S/A, sex/age, Y, year; D, disease; Sp, splenomegaly; WBC, white blood cell count; RBC, red blood cell count; Hb, hemoglobin; Ht, hematocrit; Plt, platelet count; Ph ch, Philadelphia chromosome; FUP, follow-up period. [a]pS1230F: possible polymorphism.